Theme C3: Orthotrophic steel decks

Objekttyp: **Group**

Zeitschrift: **IABSE reports = Rapports AIPC = IVBH Berichte**

Band (Jahr): **59 (1990)**

PDF erstellt am: **25.06.2024**

Nutzungsbedingungen

Die ETH-Bibliothek ist Anbieterin der digitalisierten Zeitschriften. Sie besitzt keine Urheberrechte an den Inhalten der Zeitschriften. Die Rechte liegen in der Regel bei den Herausgebern.
Die auf der Plattform e-periodica veröffentlichten Dokumente stehen für nicht-kommerzielle Zwecke in Lehre und Forschung sowie für die private Nutzung frei zur Verfügung. Einzelne Dateien oder Ausdrucke aus diesem Angebot können zusammen mit diesen Nutzungsbedingungen und den korrekten Herkunftsbezeichnungen weitergegeben werden.
Das Veröffentlichen von Bildern in Print- und Online-Publikationen ist nur mit vorheriger Genehmigung der Rechteinhaber erlaubt. Die systematische Speicherung von Teilen des elektronischen Angebots auf anderen Servern bedarf ebenfalls des schriftlichen Einverständnisses der Rechteinhaber.

Haftungsausschluss

Alle Angaben erfolgen ohne Gewähr für Vollständigkeit oder Richtigkeit. Es wird keine Haftung übernommen für Schäden durch die Verwendung von Informationen aus diesem Online-Angebot oder durch das Fehlen von Informationen. Dies gilt auch für Inhalte Dritter, die über dieses Angebot zugänglich sind.

Ein Dienst der *ETH-Bibliothek*
ETH Zürich, Rämistrasse 101, 8092 Zürich, Schweiz, www.library.ethz.ch

http://www.e-periodica.ch

Fatigue Resistance of Orthotropic Steel Decks

Résistance à la fatigue des dalles orthotropes en acier

Dauerfestigkeit orthotroper Stahl-Fahrbahnplatten

André BIGNONNET
Engineer ENSM
IRSID
St. Germain-en-Laye, France

Bernard JACOB
Civil Engineer, IPC
LCPC
Paris, France

Jean CARRACILLI
Engineer
LCPC
Paris, France

Michel LAFRANCE
GTS TFK
Dunkerque, France

SUMMARY
The present study is a part of a large European research program dealing with the fatigue behaviour of stiffener to deck-plate welded connections. A numerical model has been developed to evaluate the durability of fatigue loaded structures. Theoretical analyses have employed fracture mechanics to describe the growth of fatigue cracks. A model has been fitted with experimental results from tests of large welded specimens which were representative of a true structure. Application of the model to existing bridges leads to prediction of fatigue damage which is in agreement with problems observed in service.

RÉSUMÉ
Cette étude réalisée dans le cadre d'un programme communautaire CECA traite du comportement en fatigue de la liaison soudée tôle de platelage-auget. Un modèle numérique de prédiction de la durabilité des structures a été développé. Il s'agit d'une analyse théorique basée sur l'approche par la mécanique de la rupture de propagation des fissures de fatigue. Le modèle a été ajusté à l'aide du travail expérimental effectué sur des éprouvettes soudées soumises à des situations de contrainte rencontrées sur les structures réelles. L'application du modèle aux cas de ponts existants a conduit à des prédictions d'endommagement par fatigue cohérentes avec des désordres observés en réalité.

ZUSAMMENFASSUNG
Diese im Rahmen eines EGKS-Programmes durchgeführte Untersuchung behandelt das Ermüdungsverhalten von geschweissten Verbindungen zwischen Belagsblech und Versteifungselement. Ein numerisches Modell für die Voraussage der Dauerfestigkeit der Strukturen wurde entwickelt. Es handelt sich um eine theoretisch-bruchmechanische Analyse der Rissausbreitung. Das Modell wurde anhand von Resultaten aus experimentellen Untersuchungen geeicht. Letztere erfolgten an geschweissten Proben, die Beanspruchungen unterworfen wurden, wie sie für wirkliche Strukturen repräsentativ sind. Die Anwendung des Modells auf existierende Brücken führte zu Vorhersagen der Beschädigung, die den tatsächlich beim Betrieb beobachteten Schäden entsprechen.

1. INTRODUCTION

The fatigue strength is an important safety criterion for the steel structures such as the orthotropic decks. For that reason the European Coal and Steel Community (ECSC) has supported a wide research program for 12 years. The last phase (1986-89) was devoted to the study of the behaviour of the most sensitive details, such as the connection between the longitudinal stiffener and the plate presented in this paper. An experimental work was conducted by the IRSID in order to establish the S-N curves adapted to the actual performant welding conditions and to provide measured lifetimes under controlled loading cases. The LCPC developed a physical model of crack propagation calculation, based on the fracture mechanics theory and implemented it to the tested specimens and to some existing bridges on which measurements were done. By this way the model calibration and validation was possible and then the results concerning the bridges were compared with those by the classical S-N approach with a Miner's summation.

2. EXPERIMENTAL WORK

2.1 Type of Connection

The work undertaken dealt with the stiffener to deck plate connection. The experimental program included two aspects :

- the optimization of the welding procedure,
- the influence of an accosting gap, 0 or 2 mm, between the stiffener and the deck plate during the welding.

The specimens whose geometry is given on figure 1 are sliced from 5.50 m long assemblies. The material used is a structural steel E 36-4 (standard NFA 501-87), TMCP steel 6 mm thick for the stiffener and normalized steel 12 mm thick for the deck plate.

2.2 Welding Operation

The stiffeners have been welded in one run in horizontal position, 2F, using a submerged arc welding automatic machine, without pre-heating nor post-heating. Filler metal and flux are of the type SAF-AS35/AS462. The influence of the edge preparation has been checked, chamfered edge at 60° or 45° and without chamfer.

The welding energy has been ajusted to minimize the lack of penetration.

From these sets of welding tests, presented in more details in reference [1] it has been shown that without edge preparation, no chamfer, a satisfactory penetration (lack of penetration $\simeq$ 1 mm) is obtained for a welding energy of 20 kJ/cm, figure 2, and this even with an accosting gap of 2 mm.

2.3 Static Tests

Tests have been performed with 3 points bending as indicated in figure 1.

For a good knowledge of the strees distribution, static tests have been done on an instrumented specimen, figure 3a. It is noted that in the median axis of the specimen the loading is biaxial with $\sigma_2/\sigma_1 = 1/3$ (σ_1 is in the direction of the bending stresses).

The nominal stresses definition to be used in the fatigue S-N diagrams are derived from these tests :

- extrapolation of the stress in the deck plate to the weld-toe, figure 3b, definition generally used when the cracks propagate through the deck plate from the weld-toe,
- extrapolation of the stress in the stiffener to the weld root, figure 3c, definition generally used when cracks propagate through the weld from the root of the weld.

2.4 Fatigue Tests

Fatigue tests have been performed in alternate bending : R=-1 ($R = S_{min}/S_{max}$).

The results are expressed in terms of the nominal stress range in the deck plate as defined above, $R = S_{max} - S_{min}$, versus the number of cycles to failure.

Two different criteria have been used in the presentation :

N_1= crack detection by extensometry, a ≃ 0.3 mm (see reference [1]).

N_4= end of test (large displacement of the actuator).

The welding procedure used leads to a lack of penetration lower than 1 mm and a throat of about 6 mm. With these conditions for R = -1, the cracks initiate systematically in the deck plate at the weld toe.

The results given in figure 4 show that for the welding conditions used there is no difference in fatigue behaviours between a stiffener welded with a gap of accosting of 2 mm and a stiffener welded without gap. The whole results with R = -1 lead to a Wöhler curve, figure 4, such as ΔS (MPa) = 26477 $N^{-1/3}$, standard deviation = 24 MPa.

On figure 5, these results are compared with those from Liège University [2] and from CRIF [3], for comparable R ratio (between -0.57 and -1) in terms of nominal stress range in the stiffener at the weld root. The primarily difference with IRSID results is that experiments of Liège University [2] and CRIF [3] show a crack initiation at the weld root, and the failure occurs in the weld. As shown in table 1, the specimen used at CRIF [3] welded by manual arc welding involve an important lack of penetration.

It is clear from figure 5 that the fatigue strength significantly increases when using submerged arc welding, this technique allows larger penetration and larger throat of the weld. Nevertheless, it is shown that cracks initiate at the weld of the root for a lack of penetration larger than 2 mm. Conversely if the welding operation is properly optimized the lack of penetration can be limited at about 1 mm and for alternate or repeated tensile bending in the deck plate the crack initiate at the weld toe, and the fatigue strength is improved. This is interesting for the purpose of inspection and structure safety. If the lack of penetration remains of the order of 1 mm, the risk of fatigue cracking is reported at the weld toe which is more accessible to control.

References	Lack of penetration (mm)	Throat (mm)
this work	1 to 1.5	5.5 to 6.5
[2]	2 to 2.5	5 to 6
[3]	3 to 4.5	3.5 to 4.5

Table 1 : Geometric welds characteristics, presented here and references

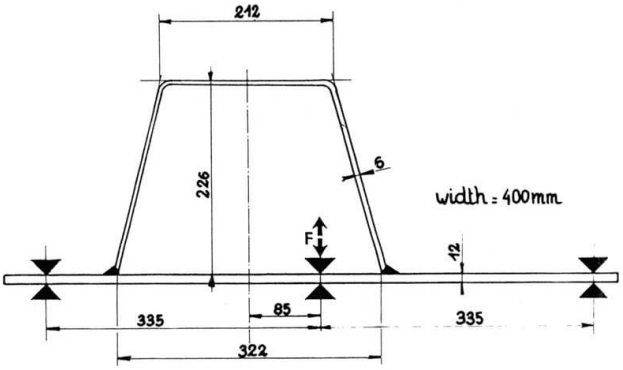

Fig.1 : Geometry of the specimen

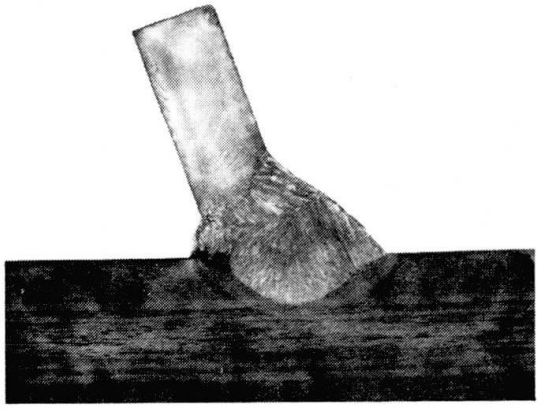

Fig.2 : Macrography of the weld

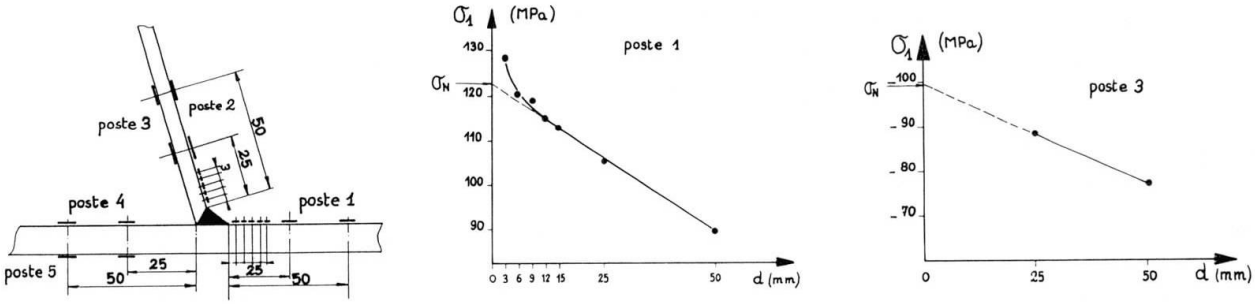

Fig.3 : Gauge instrumented specimen a), and nominal stress definition in the deck plate b) and in the stiffener c).

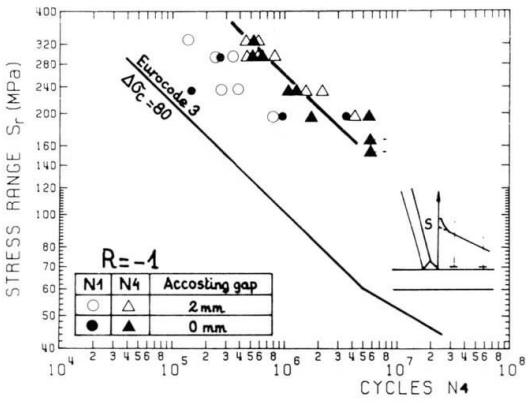

Fig.4 : Wöhler curve at R=-1 for two accosting gaps, on the basis of the stress range in the deck plate.

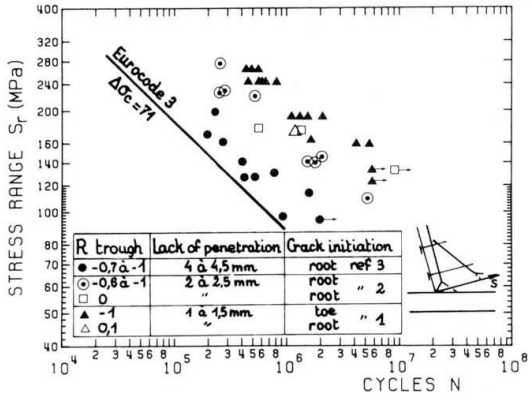

Fig.5 : Comparison of fatigue results with litterature data, on the basis of of the stress range in the stiffener.

3. FRACTURE MECHANICS ANALYSIS

3.1 Model of Damage

The classical fatigue S-N calculation with a Miner's summation, generally used by the engineers, remains the basis of most of the codes. But the strong assumptions about the linear damage accumulation, which does not take into account the stress variation time history, make this approach very poor and far from the real crack propagation phenomena.

The fracture mechanics applies the principles of the continuum mechanics to describe the crack propagation. The stress distribution is analysed in detail around the crack end. Here, only the mode I - crack opening - is considered, and the propagation time is computed. The time of crack initiation is not taken into account because it is assumed that the local surface defects already provide small cracks. This initial state is summarized by a conventionnal crack length a_0.

3.2 Propagation Law

The crack propagation is governed by the stress intensity factor K, which characterizes the local geometry of the structure and the effect of a stress variation on the crack growth rate. Between the many models proposed, we have chosen the Paris law with a threshold, one of the simplest but realistic models. The crack growth rate is given by :

$$\frac{da}{dN} = C(\Delta K - \Delta K_S)^m \qquad (1)$$

where da is the elementary increase of the crack length under dN stress variation cycles, C and m are two constant parameters which characterize the material ; ΔK_S is a threshold of non propagation. The increase of the stress intensity range under a stress variation $\Delta\sigma$ may be written :

$$\Delta K = K_M - K_m = \sqrt{\Pi a}\ \Delta\sigma\ f(a) \qquad (2)$$

where f(a) is a magnification factor representing the local geometry.

Finally, the lifetime is obtained by integration of (1) :

$$N = N_0 + \frac{1}{C}\int_{a_0}^{a_r} \Delta K^{-m}\, da \quad , \text{ where } a_r = e/2 \text{ is the failure criteria} \qquad (3)$$

e beeing the plate thickness.

3.3 Calculation of the Stress Intensity Factor

If the stress diagram $\sigma(x)$ in the non-cracked section is expressed as a polynom of x :

$$\sigma(x) = A_0 + A_1 x + A_2 x^2 + A_3 x^3 + A_4 x^4 \qquad (4)$$

then the stress intensity factor of equation (2) may be written as :

$$K = \sqrt{\Pi a}\ \left[A_0 F_0 + \frac{2a}{\Pi} A_1 F_1 + \frac{a^2}{2} A_2 F_2 + \frac{4a^3}{3\Pi} A_3 F_3 + \frac{3a^4}{8} A_4 F_4\right] \qquad (5)$$

where the F_i are the magnification factors, functions of a, the present crack length. They are calculated using a superposition principle and the successive

application of simple stress diagrams, and for a finite set of values of a. A finite element method is used in this determination. As an example, F_0 and F_1 are plotted as functions of a in the figure 6.

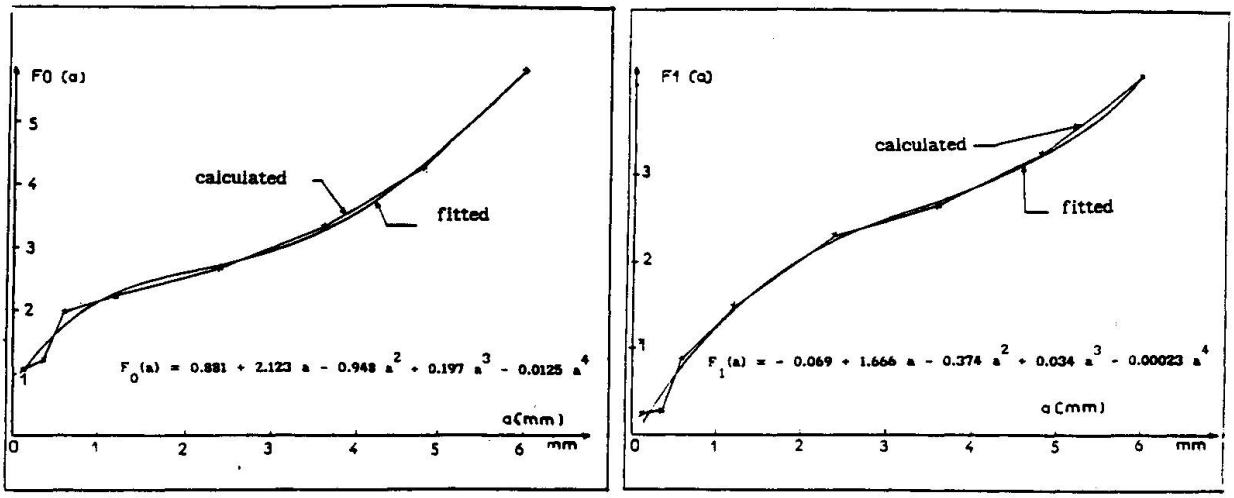

Fig. 6 Magnification factors F_0 and F_1

4. APPLICATION TO EXISTING BRIDGES

The part considered is the longitudinal welded connection between the stiffener and the plate of the orthotropic decks. It is one of the most sensitive element to fatigue damage. Several cracks have already been found in some existing bridges, especially for thin plates of 10 mm [4].

4.1 Crack Propagation Calculation

The crack is located in the plate, in a plane which is perpendicular to its surface and which contains the weld. The magnification factors are calculated as explained in the § 3-3.

The stress time history, measured by strain gauges on the bridges under a real traffic or computed by the LCPC's program CASTOR [5] by using the influence surface and a traffic record made by piezo-electric cables [6], is summarized in an histogram for a reference period T (generally T = 1 week). If N_i and N_c are the number of stress cycles with an amplitude σ_i and the total number of cycles by time unit, equations (1), (2) and (5) give :

$$da = \sum_{i=1}^{N_c} f(a,\sigma_i) N_i \, dt \quad , \text{ or } \quad da_{n+1} = \varepsilon\, a_n = \sum_{i=1}^{N_c} f(a_n,\sigma_i) N_i \, dt_{n+1} \tag{6}$$

after discretization, and with $a_r/a_0 = (1+\varepsilon)^j$; j corresponds to the total number of time steps when the failure occurs ($a = a_r$). The total lifetime is :

$$D = a_0 \sum_{k=1}^{J} \frac{\varepsilon\,(1+\varepsilon)^k}{\sum_{i=1}^{N_c} f(a_0(1+\varepsilon)^k,\sigma_i) N_i} \tag{7}$$

A computer program PROPAG [1] was written in order to compute this lifetime and to provide the crack evolution.

4.2 Model Calibration

The crack propagation calculation was first applied to the test specimens presented in the § 2, in order to calibrate some parameters and to check its results. A finite elements calculation made on the structure with the real loading and boundary conditions provided the stress diagram in the section of the plate :

$$\sigma(z) = 157.21 - 55.82\ z + 8.93\ z^2 - 0.866\ z^3 + 0.029\ z^4 \qquad (8)$$

The crack length increases were recorded during the tests for two stress amplitudes (200 and 300 MPa), and the coefficients C and m of (1) have been fitted to the results. They were found close to those proposed in the litterature and finally adopted : $C = 8.10^{-12}$, and $m = 2.85$, for ΔK in MPa $\sqrt{m}$ and da/dn in m/cycles.

In the tests we used the ratio $R = \sigma_{min}/\sigma_{max} = -1$. Because it was shown by other tests that the lifetime is highly dependent on this ratio and that only the tensile stresses allow to increase the crack, the stress amplitude taken into account here was $\sigma/2$.

The results of the calculation are compared with the experimental ones for several nominal stress from $\Delta\sigma = 200$ MPa to $\Delta\sigma = 340$ MPa, each time with 5 initial crack lengths between 0.05 mm and 0.4 mm (table 2). It is easy to conclude that an appropriate initial crack length under these welding conditions is 0.1 mm.

$R = \frac{\sigma_M}{\sigma_m}$	$\Delta\sigma$ (MPa)	Number of cycles at failure (IRSID tests)	Fracture mechanics model	
			a_0 (mm)	N. of cycles at failure
-1	200	2031000 729000 3443000 m= 2068000	0.05 0.10 0.15 0.20 0.40	3166000 1608000 1052000 777900 399900
-1	240	1076000 1274000 1767000 m= 1372000	0.05 0.10 0.15 0.20 0.40	1884000 957000 626000 463000 238000
-1	300	315000 548000 m = 431500	0.05 0.10 0.15 0.20 0.40	998000 507000 332000 245000 125900
-1	340	350000	0.05 0.10 0.15 0.20 0.40	698000 355000 232000 172000 88100

Table 2 : Comparison of the tested and computed lifetimes

4.3 Lifetimes of Existing Bridges

We present here the application of our model to the connection between the plate and the longitudinal stiffener for three cases of orthotropic deck bridges. Two of these bridges are temporary structures with a thin plate of 10 mm and a 6 mm thick stiffener (Montlhery and Choisy). The third one is the large box-girder bridge of Caronte, with a main span of 130 m and a total length of 300 m. The plate thickness is 12 mm.

In the cases of Caronte and Montlhery, the stress variations were measured under the traffic loads during previous phases of a ECSC's contract [7], by strain gauges sticked close and perpendicular to the weld. The nominal stress is obtained by a linear extrapolation, from two other points. In the case of Choisy, the stress variations are calculated by the program CASTOR, using the measured influence surface and the recorded traffic loads. The calculation is done with two traffics : the real one (RN 305) and the traffic of the RN 23 which is heavier and denser, in order to predict the consequences of an increase of the loads and traffic density.
The stress diagrams are for Montlhery and Choisy :

$$\sigma(z) = 7.533 - 2.706\ z + 0.481\ z^2 - 0.0788\ z^3 + 0.0055\ z^4 \qquad (9)$$

and for Caronte : $\sigma(z) = 6.024 - 3.287\ z + 1.075\ z^2 - 0.19\ z^3 + 0.0123\ z^4$ (9')

Due to the high residual stresses, all the stress variations under traffic loads are assumed to be in the tensile domain and hence are taken into account. The threshold of non-propagation ΔK_s has been chosen in accordance with the fatigue limit of the ECSC's S-N curves [8]. An initial crack length of 0.3 mm has been adopted corresponding to the welding conditions of these structures.

In all cases, the lifetime calculations were made by our fracture mechanics model and by the classical S-N curves and Miner's summation. The results are presented and compared in the table 3. The relevant S-N class for our element is 50 at least for the thin plates ; for Caronte the class 63 or 71 can be used. The figure 7 shows the crack evolution in the time in all cases ; a conservative choice of ΔK_s, which corresponds to the class 50, was made. This non-linear evolution is clearly different as the S-N approach. The lifetimes obtained by our model are slightly longer than those by S-N calculation, but, above all, the sensitivity to the S-N class is much lower, which seems to be more realistic.

CLASS	MONTLHERY		CARONTE		CHOISY Traffic RN 306		CHOISY Traffic RN 23	
(ECSC)	S-N	F.M.	S-N	F.M.	S-N	F.M.	S-N	F.M.
36	6	30	37	188	26	107	6	24
40	8	31	57	218	37	112	8	26
45	14	34	99	269	60	121	13	28
50	21	38	172	371	92	132	21	30
56	33	44	315	∞	138	147	31	34
63	55	55	600	∞	224	176	51	42
71	103	78	1393	∞	401	234	94	59

Table 3 : Computed lifetimes (in years) of existing bridges and comparison with S-N approach.

5. CONCLUSIONS

Two important points can be pointed out :

1/ From the manufacturing point of view it is clear that with a properly optimized automatic welding, improved fatigue resistance can be easily obtained. Therefore, taking into account the modern production tools, widely used in the european industry, it appears that the actual regulations are somewhat too conservative.

2/ From the point of view of the reliability of the structures we have shown that the physical approach of the fatigue for steel bridges can be made with a simple model which gives realistic fatigue lives, and with a lower scattering than with the classical S-N approach. The numerical program developped together with finite elements codes available, allows to make this type of calculation on a micro computer.

This study and parallel works done within the framework of the ECSC program show that the evaluation of the reliability of our bridges and the competitiveness of the steel structures still improve.

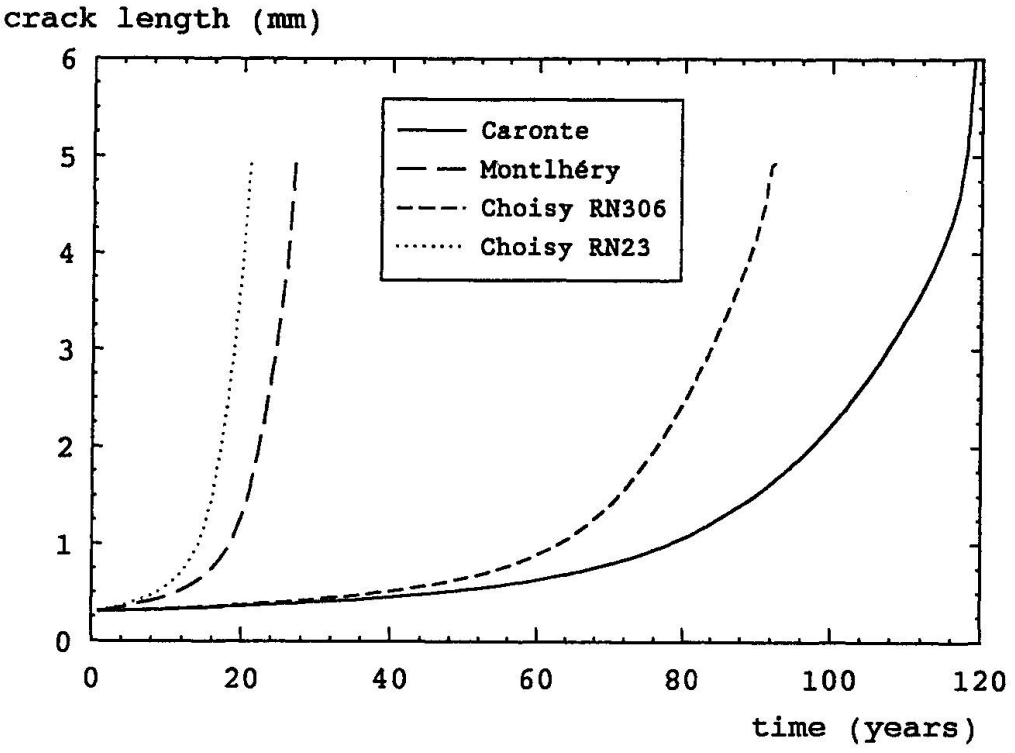

Fig. 7 : CRACK GROWTH

REFERENCES

1. BIGNONNET A., CARRACILLI J., JACOB B., Comportement en fatigue des ponts métalliques. Application aux dalles orthotropes en acier. Rapport final convention CECA, 7210 KD 217, Août 1989.

2. BRULS A., POLEUR E., Résistance à la fatigue des dalles en acier des ponts-routes. Rapport final convention CECA, KD 201, Avril 1989.

3. THONNARD, JANSS, Comportement en fatigue des dalles orthotropes avec raidisseurs trapézoïdaux. Rapport CRIF, MT 161, Août 1985.

4. MEHUE P., Fissures de fatigue dans les viaducs métalliques démontables, 13e congrès AIPC, Helsinki, juin 1988.

5. EYMARD R., JACOB B., Le programme CASTOR pour le Calcul des Actions et Sollicitations du Trafic dans les Ouvrages Routiers. Bull. liaison des LPC, n° 164, novembre-décembre 1989.

6. JACOB B., Connaissance du trafic routier et des sollicitations induites dans les ouvrages. Annales de l'ITBTP, n° 478, novembre 1989.

7. JACOB B., CARRACILLI J., Mesure et interprétation des charges dynamiques dans les ponts - Etude de la fatigue. Rapport final convention CECA, 7210 KD 311, juillet 1983.

8. Convention Européenne de la Construction Métallique, Recommandations pour la vérification en fatigue des structures en acier. Construction Métallique, n° 1 - 1987.

Fatigue Behaviour of Field-Welded Rib Joints in Orthotropic Steel Bridge Decks

Comportement à la fatigue des connexions de raidisseurs soudés dans des dalles orthotropes de ponts en acier

Ermüdungsverhalten in situ geschweisster Rippen orthotroper Stahlfahrbahnplatten

Henk KOLSTEIN
Research Engineer
Delft Univ. of Technology
Delft, The Netherlands

Henk Kolstein, born 1952, joined the Delft University of Technology in 1971. He is involved in research in steel structures at the Stevin Laboratories, investigating static and fatigue behaviour of bolted and welded joints. Since 1978, he has been participating in ECSC research within the domain of bridge loading and fatigue of orthotropic steel decks.

Jacobus DE BACK
Professor
Delft Univ. of Technology
Delft, The Netherlands

Jacobus de Back, born 1924, joined the Delft University of Technology in 1951. He was nominated as Professor of steel structures in 1972. Since 1957, he has been involved in research in steel structures. He is a member of several technical and standardization committees in The Netherlands and international committees of ECSC, ECCS, IIW and CIDECT.

SUMMARY
This paper describes the results of several research programs related to fatigue behaviour of field-welded rib joints in othotropic steel bridge decks. Constant as well as variable amplitude tests were carried out on several connections. Eurocode 3 fatigue design lines are considered. Fatigue cracks growing from welded details in an existing bridge and subsequent activities are reported. Finally, a fatigue design method which uses standard design curves and influence lines related to the static design load is introduced.

RÉSUMÉ
Cet article présente les résultats de plusieurs programmes de recherche relatifs au comportement à la fatigue des connexions de raidisseurs soudés dans des dalles orthotropes de ponts en acier. Des essais de fatigue sous amplitudes constante et variable ont été effectués sur différents types de connexions. Les courbes de fatigue de l'Eurocode 3 ont été considérées. Des fissures de fatigue apparues dans des détails soudés de ponts existants sont présentées, ainsi que les actions entreprises pour y remédier. Finalement, une méthode de calcul utilisant les courbes de Wöhler standardisées et les lignes d'influence relatives au modèle de charge statique est introduite.

ZUSAMMENFASSUNG
Dieser Artikel stellt die Resultate verschiedener Forschungsprogramme vor, die das Ermüdungsverhalten auf der Baustelle geschweisster Rippen orthotroper Fahrbahnplatten von Stahlbrücken betreffen. Verschiedene Arten solcher Verbindungen wurden sowohl unter konstanter als auch variabler Amplitude getestet. Dabei wurden die im Eurocode 3 enthaltenen Ermüdungsfestigkeitskurven berücksichtigt. Über Ermüdungsrisse, die in bestehenden Brücken von geschweissten Konstruktionsdetails ausgehen, wird ebenso berichtet, wie über die in solchen Fällen zur Auswahl stehenden Instandstellungsmassnahmen. Schliesslich wird eine Methode für die Ermüdungsbemessung vorgestellt, basierend auf normierten Wöhlerkurven und Einflusslinien in Verbindung mit den statischen Bemessungslasten.

1. INTRODUCTION

In most large orthotropic steel bridge decks, field splices are necessary because transportation of the complete bridge from the shop to the site is seldom possible. In general, both longitudinal and transverse field splices have to be made. In the longitudinal splices, only the deck plate has to be connected. This is mostly done by butt welding and as the weld is accessible both from above and from below, a good quality of the weld can be achieved. The same applies to the transverse butt splice weld in the deckplate. At the transverse splice the longitudinal ribs have to be connected as well.
With closed ribs, mostly used in modern bridges, the most appropriate way of splicing is by welding but as the welds can only be made from the outside in an unfavourable overhead position, the quality of those welds will be dubious. Depending on the location of the splice in the deck, the load on the splice can have a fluctuating part due to the traffic load, dominating the static loading, so conditions for fatigue damage are present.
As the splice in the ribs frequently occurs in a bridge deck, an investigation of the fatigue behaviour of field splices is worth while. Besides cracks were discovered in several field welded splices in a rib of a bridge which was 15 years in duty.

2. FATIGUE TESTS ON FULL SCALE TEST SPECIMENS

In this paper, the results of the fatigue tests are plotted in a S-N-diagram on a log-log scale. The regression mean-line minus twice the standard deviation is used to make comparisons with the fatigue design curves, defined by the Eurocode 3.

2.1. Constant amplitude tests

2.1.1. Dutch research

In 1974 [1], a research programme was set up to investigate the design of field splices in orthotropic steel bridge decks with respect to economy and fatigue strength. Laboratory tests were conducted at IBBC-TNO and at the Stevin Laboratory. The specimens for the bending tests were single trapezoidal rib specimens 2/325/6, steelgrade Fe 510. Three types of field splices were selected, as shown in figure 1.

- Type A : Butt splice with back-up strips (4 mm root gap)
- Type B : Lap splice with fillet welds
- Type C : Butt splice with a thick joint plate.

The conclusion (fig.1) can be drawn that the fatigue behavior of type C is the best (EC 125) and of type B is the worst (EC 56), with type A in between (EC 80). Nevertheless, with respect to type C, it must be noted that apparently this type is very sensitive to the quality of the workmanship, for the first series of specimens made with less care gave very bad results. That is one of the reasons why type A is often used.

As all tests were carried out at high stress range levels ($\geq$ 120 MPa), where the shape of the S-N curve amounts 3, no information is available at the lower stress regions and on the fatigue limit. This stress range region is very important, for measurements carried in ECSC research [2,3] showed for this type of connection a maximum stress range of $\pm$ 80 MPa.

In 1986 [4], an ECSC research program started at the Stevin Laboratory in which among other things, constant amplitude tests were carried out on the type A

detail at stress ranges beyond 2.10^6-3.10^7 cycles. Besides, the effect of the root-gap of the weld has been examined by varying the gap between the stiffener and the splice in 0, 2 and 4 mm. Furthermore tests were executed with an improved form of the weld (V-groove). The fatigue results are gathered in figure 2.

For the specimens with a root gap of 4 mm it appears that, the specimens tested at stress ranges > 120 MPa fall within the spread band of the previous tests [1]. At 105 MPa the fatigue strength is far more than one would expect. The fatigue cracks appeared over 9 million cycles instead of about 3 million cycles. The specimen tested at a stress range level of 90 MPa did not fail after almost 30 million cycles.
Comparing the results it appears furthermore, that a weld with a root gap of 0 or 2 mm can result in a fatigue strength far below the strength of the weld with a root gap of 4mm (a factor 12 - 18).
Changing the weld geometry by using a V-groove did not give the expected improvement.

2.1.2. Comparison with foreign research

In 1988 an Japanese IIW document [5] was published which contained, analogous to the Dutch researches [1,4], fatigue results on trapezoidal ribs. Also in this research, a great influence of the largeness of the root gap on the fatigue strength was found. Summing up these two test programmes, it can be concluded that Class 71 according the Eurocode 3 can be recommended for field splices type A, with a root gap ≥ 3 mm (fig.3a). If the root gap < 3 mm the classification decreases to a Eurocode Class 36 (fig.3b). Naturally it is better to avoid the last situation, but it is known that some of the existing bridges contain the type A detail with very small root gaps.

Simultaneous to the Dutch ECSC research [4] the Italian partners in this joint ECSC research investigated the fatigue behaviour of field splices in ribs of orthotropic decks [6]. They studied a triangular shape of the trough instead of a trapezoïdal one. Following details were tested (fig.4a):
- Butt splice using a V-groove with a root gap of 6 mm and a backing strip.
- Butt splice using a X-groove with a root gap of 4 mm, without backing strip.

From the results as given in figure 4a it can be concluded, that the V-groove specimens conducted better than the X-groove type. In both cases the behaviour is better than the Dutch [1,2] and Japanese [3] researches. However it must be noticed that all the welding of the Italian research have been checked by means of visual and magnetic controls. The butt welding, moreover, have been 100% X-rayed and repaired if necessary.

A triangular shape was also studied in the United Kingdom [7] in 1982. The following details were tested (fig.4b):
- Butt splice with backing strip and a root gap of 12 mm.
- Three series of butt splices with a sealing plate of 19 mm. The welding procedure as well as the influence of stress relieving was studied.

From the results as given in figure 4b it can be concluded that the fatigue strength of these testspecimens is comparable with those of the Italian research. Besides, the behaviour of the welded connections with a sealing plate of 19 mm is better than the one with a backing strip (Type E).

Gathering the Italian and UK-tests together, it can be noticed that perhaps for the triangular shapes containing a weld with backing strip and a root gap of 6 - 12 mm, a Eurocode Class 112 can be considered (fig.4c).

2.2. Variable amplitude tests

In above mentioned Dutch ECSC programme [4], also some variable tests were carried out. Special attention was performed to long life (low stress) fatigue results and testing the Miner summation by comparing variable and constant amplitude tests.

2.2.1. Load-spectra for the variable amplitude test.

Axleload-spectra and stress-spectra measured in the ECSC-research [2,3] together with the computer assessment programme of the University of Liege, were used. For the computer simulation , the traffic flow of the Rheden Bridge and a theoretical influence line were used to simulate a test-load spectra for the field splice in a longitudinal rib. Analysis of the simulated spectra showed, that the low stress ranges cause only 7% of the total damage of the spectra. These stress range classes amounts however 84 % of the total number of cycles (fig.5a). So leaving out these classes, resulted in a 'reduced spectrum' saving a lot of testing time without attacking the potential fatigue damage of the spectrum (fig.5b).
Besides the above mentioned simulated test-load spectrum, for one of the specimens a measured stress-spectrum was used. This spectrum (fig.6) was measured on the the Forth Bridge in the United Kingdom [2,3]. Considering the constant amplitude tests the stress range level of the actual measured and simulated were raised to a higher level for the variable amplitude tests.

2.2.2. Analysis of the spectra using Miner

To compare the variable amplitude test results with the constant amplitude ones, the applied stress-spectra were analyzed in two different ways.

a. An equivalent stress range $\Delta\sigma_e$ was calculated in a way that n-cycles of that stress range have the same fatigue damaging potential as n-cycles of the stress-spectrum, using a third power relationship;

$$\Delta\sigma_e = \left(\frac{1}{n_i} \Sigma n_i \Delta\sigma_i^3\right)^{1/3} \text{ MPa.}$$

b. The University of Liege proposed [3] the following equivalent stress $\Delta\sigma_m$ and belonging number of cycles n_m;

$$\Delta\sigma_m = \frac{\Sigma n_i \Delta\sigma_i^3}{\Sigma n_i \Delta\sigma_i^4} \text{ MPa} \quad \text{and} \quad n_m = \frac{\Sigma n_i \Delta\sigma_i^3}{\Delta\sigma_m^3}.$$

In these formulae : $\Delta\sigma_i$ = individual stress range

n_i = individual number of cycles belonging to $\Delta\sigma_i$

$\Delta\sigma_m$ = equivalent stress range

n_m = number of cycles belonging to $\Delta\sigma_m$.

In this paper both methods are be used (fig. 5 and 6).

The fatigue results of the variable amplitude tests are presented in figure 7. It appears, that there is a very good agreement between the constant amplitude tests and the variable amplitude tests using the Miner calculation. Furthermore no cracks were found in the specimen with a maximum stress range of the spectrum of 132 MPa after testing for 48 million cycles. Comparing the results of the tests applying the "measured-stress-spectrum" and the "simulated stress-spectrum", the difference seems to be very small.

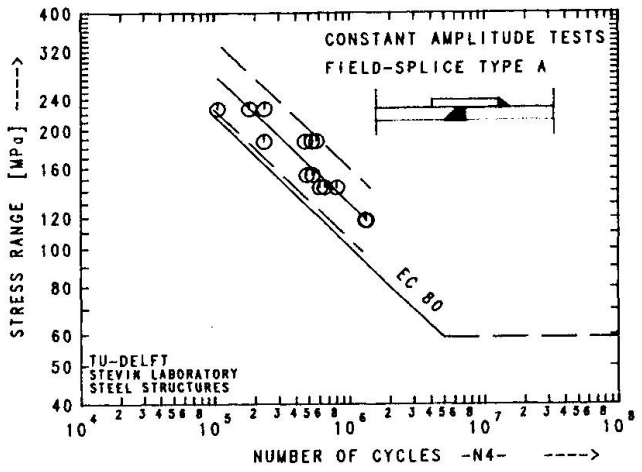

-1a-

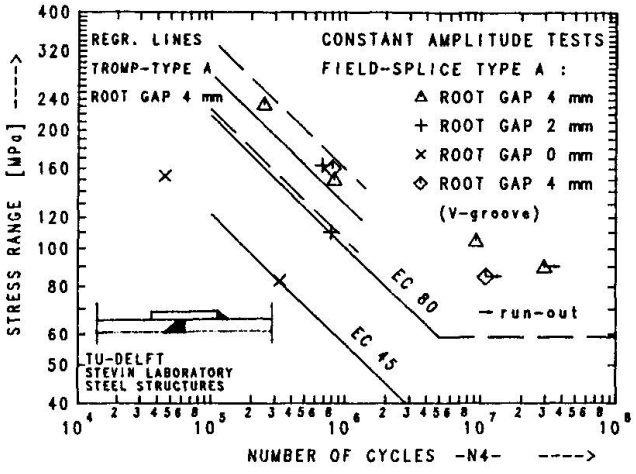

Test results Kolstein [Ref.4.]
Figure 2.

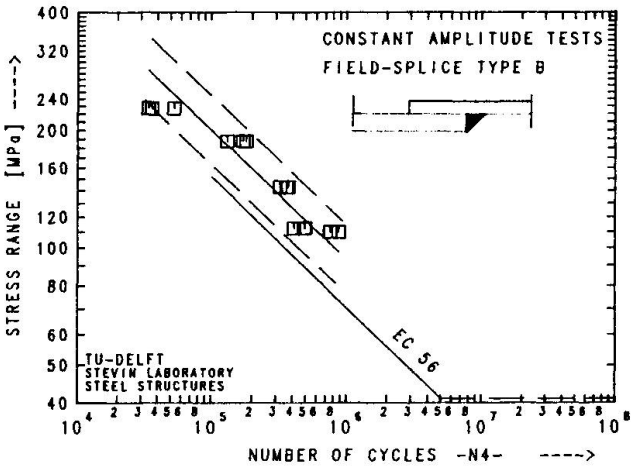

-1b-

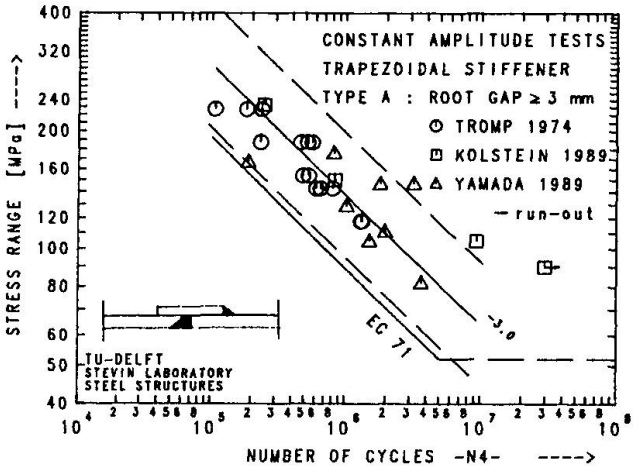

-3a-

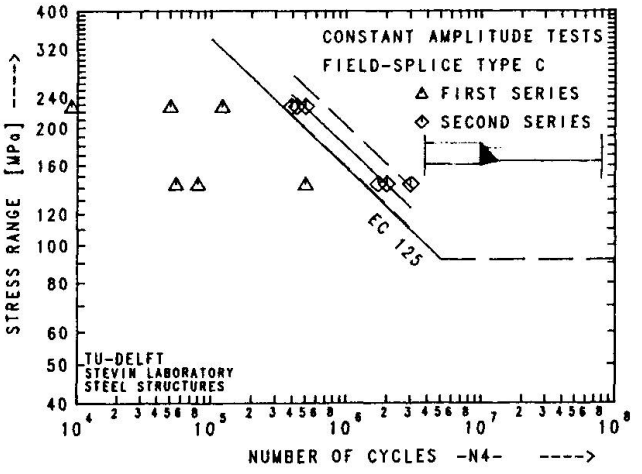

-1c-
Test results by Tromp [Ref.1].
Test results by Kolstein [Ref.4].
Figure 1.

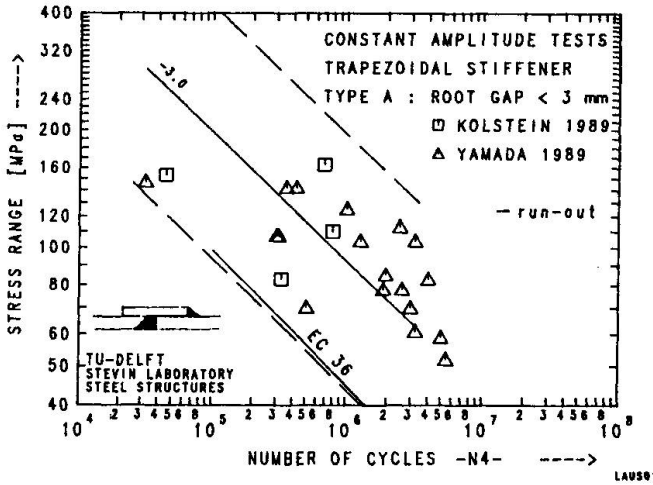

-3b-
Comparison test results; Tromp, Kolstein and Yamada [1,4,5].
Figure 3.

3. FATIGUE CRACKS IN AN EXISTING BRIDGE

During the course of routine maintenance work on the Muiden Bridge in 1985, in one of the 68 longitudinal ribs, cracks were found in several field-welded splices. For some of these connections about 70% of the total cross-section was cracked. The rib splice detail is similar to the type-A detail with a root gap of 2 mm. Due to the fact this bridge was used for only 15 years and the specific detail had been used in a lot of other bridges a research was urgently needed.

Calculations and measurements were executed to find reasons for this cracks and the remaining fatigue life of the bridge [8]. The fatigue calculations are made by using at first a derived load spectrum and in the second place a measured stress-spectrum for this detail.

3.1 Traffic loading during 15 years

Since the opening of the Muiden Bridge in 1970, traffic measurements had been carried out. These measurements concerned the counting of the vehicles. Three categories of vehicles are considered:
- B1: Light-weight vehicles (a passenger car, a delivery van, a motor-cycle),
- B2: Rigid commercial vehicles (a bus, a rigid truck without trailer),
- B3: Articulated commercial vehicles (a rigid truck and trailer, a trailer truck).

In the period 1970 - 1985 a total of $1,07.10^7$ vehicles was counted.

Using measurements from ECSC research [2,3], the following distribution of categories B2 and B3 over the fast and slow lane could be derived:

TYPE	TOTAL: $1,07.10^7$	FAST LANE	SLOW LANE
B2	4,2% → $4,5.10^6$	18% → $0,8.10^6$	82% → $3,7.10^6$
B3	2,9% → $3,1.10^6$	23% → $0,4.10^6$	87% → $2,7.10^6$

The number of axle loads ≥ 10 kN (N10) in the Slow Lane amounts 3,5 times the number of trucks B2 and B3, which results in N10 = $2,2.10^7$.

3.2. stress-spectrum of the field splice in a longitudinal rib

Relating the measured axle load spectra and stress-spectra of the Forth Bridge (fig.6) it appeared, that the number of stress range cycles ≥ 10 MPa (NR) is equal to 0,42.N10. That means for the Muiden Bridge a number NR = $0.928*10^7$. Assuming as a first approach that 10 kN wheel load results in a stress range of 15 MPa for the considered field splice, a stress-spectrum based on an load spectrum for the period 1970 - 1985 was determined. For the first fatigue calculation the measured axle load spectrum from the Rheden Bridge was used (SPECTRUM-I). A second fatigue calculation was made using directly the measured stress-spectrum of the Forth Bridge. In this case the number NR is the same as with the first calculation (SPECTRUM-II).
In figure 8 both stress-spectra and the Eurocode S-N curve EC 80 are plotted.

3.3. Calculated fatigue lives

Using Miner the following life-times could be calculated:
- SPECTRUM-I : Load spectrum Rheden Bridge and 10 kN → 15 MPa : 13,3 years,
- SPECTRUM-II: stress-spectrum Forth Bridge : 55,5 years.

The longer fatigue life of the second calculation is perhaps too optimistic because the measured axle loads in the United Kingdom are lower than in the

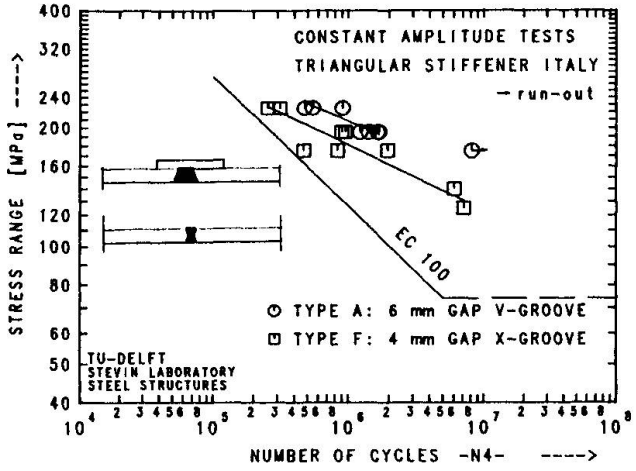

-4a-

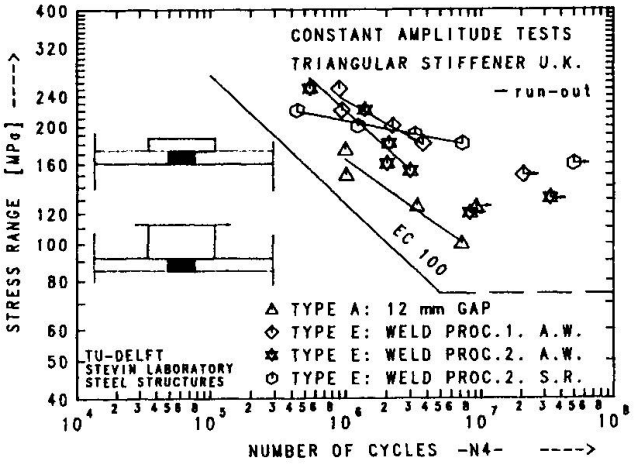

-4b-

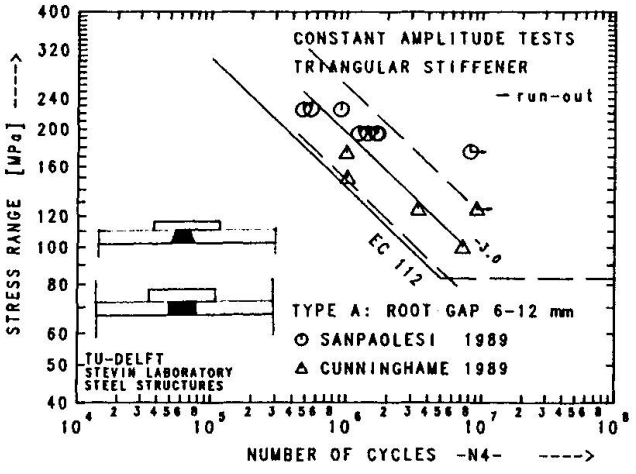

-4c-

Test results Sanpaolesi [Ref.6] and Cunninghame [Ref.7].
Figure 4.

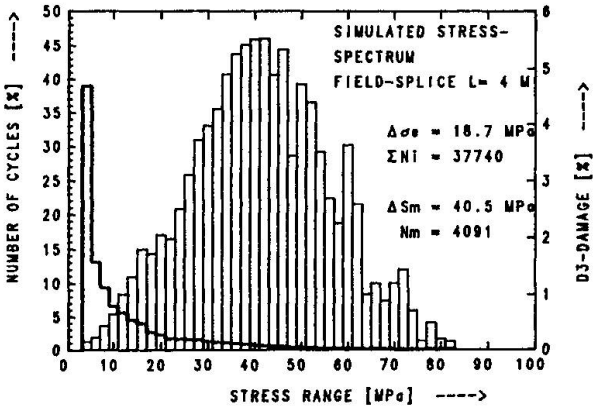

-5a-

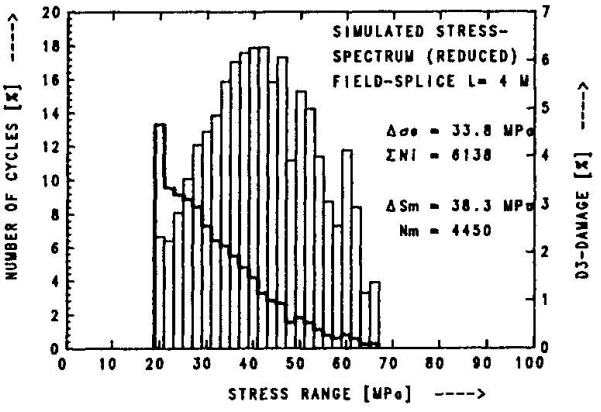

-5b-

Simulated stress spectra [Ref.2,3].
Figure 5.

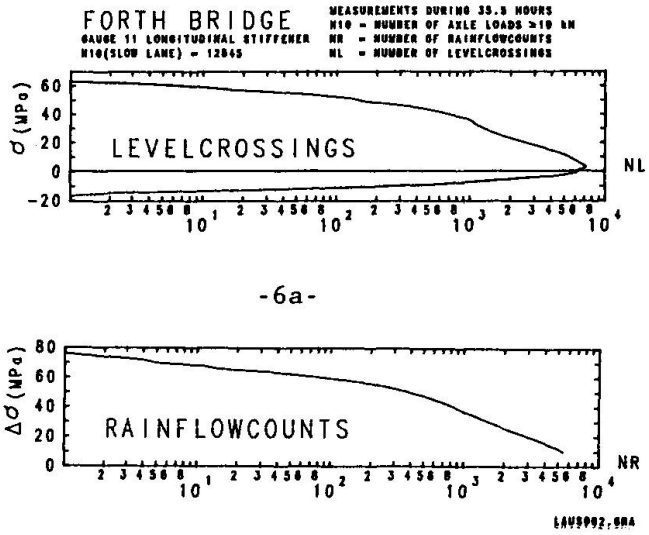

-6a-

-6b-

Netherlands (fig.9). At this stage of the research it was clear that the cracks and fatigue calculation agree, which was a very unlucky situation.
To check the assumed relation load-stress, strain measurements on the Muiden Bridge were carried out.

3.4. Strain measurements

Strain gauges were fixed on several longitudinal ribs to check if the damaged rib was the most heavily loaded one. Three types of measurements were carried out:

- Measurements without interrupting the the real traffic,
- Static measurements with a calibrated truck,
- Dynamic measurements with a calibrated truck.

The analyzed stresses by counting levelcrossings are given in figure 10. It can be seen that the measured stresses on the Muiden Bridge are little lower than those measured on the Forth Bridge and the damaged rib (gauge 2) had to sustain the highest stresses.

The results of the measurements with the calibrated truck are summarized as follows:

static	front wheel	10 kN → 11,8 MPa
	rear wheel	10 kN → 10,0 MPa
dynamic	front wheel	10 kN → 7,9 MPa
	rear wheel	10 kN → 7,5 MPa

It is clear that the assumption of 10 kN wheel load resulting in a stress of 15 MPa is not realistic for this detail.

3.5 Second series of fatigue calculations

Using the load spectrum of the Rheden Bridge a second series of fatigue calculations was made. The results are summarized below:

- SPECTRUM III : 10 kN → 12 MPa : 28,6 years
- SPECTRUM IV : 10 kN → 10 MPa : 66,0 years
- SPECTRUM V : 10 kN → 8 MPa : 145,6 years

It can be concluded, that the calculated fatigue life for the field splice in the longitudinal rib of the Muiden Bridge is much longer than 15 years. Knowing that the calculations were made in the most unfavorable situation, all wheel loads in the same track, the number of years must be higher.

3.6 Quality of the welds

Examination of cracks showed, that the quality of the welds was very bad. It was concluded that the very bad execution of the welds was the main reason for the observed cracks in this detail. However it must be remembered that the root gap of the detail in this bridge was 2 mm and with the knowledge of the later executed laboratory tests [4,5], it is clear that the EC 80 is too high and more cracks are not excluded in the future.

4. FATIGUE DESIGN USING STANDARD FATIGUE DESIGN CURVES [9,10]

When the static design stresses $\Delta\sigma st$ are known, there is a possibility to have a relationship to the actual stress ranges due to real traffic. The actual stress ranges can be expressed in a proportion of the stress range $\Delta\sigma st$. This opens the way to investigate the fatigue problem for existing bridges but also

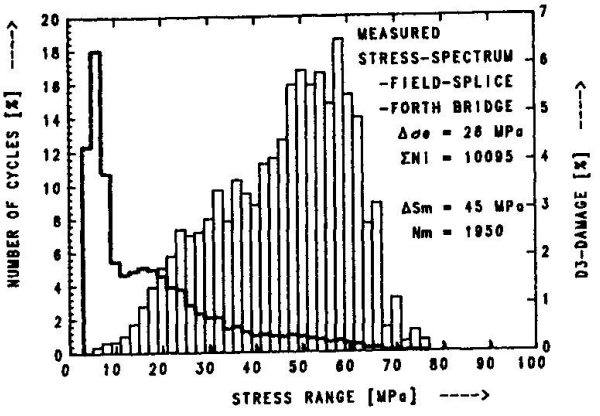

-6c-

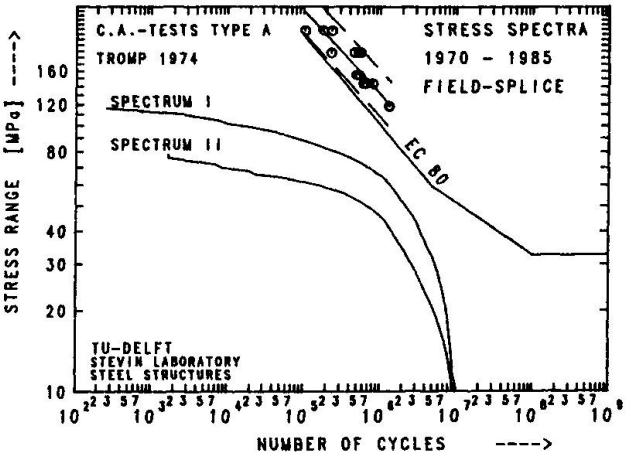

Stress spectra Muiden [Ref.8].
Figure 8.

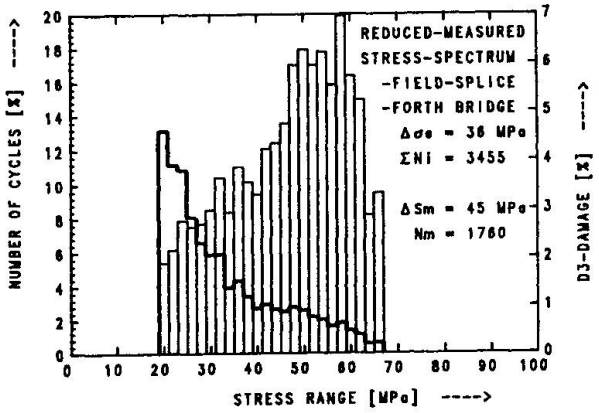

-6b-
Measured stress spectra [Ref.2,3]
Figure 6.

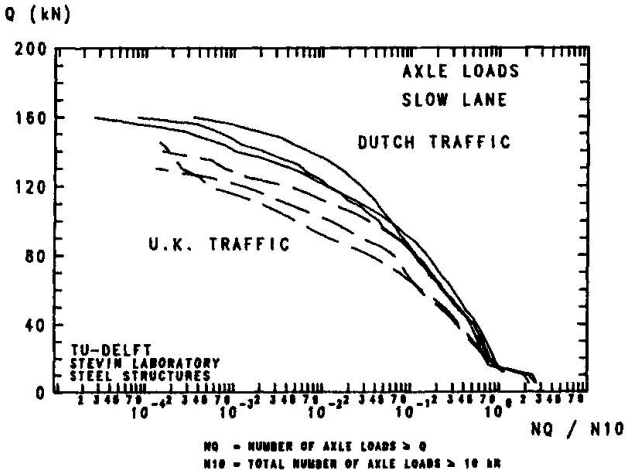

Axle load spectra [Ref.2,3].
Figure 9.

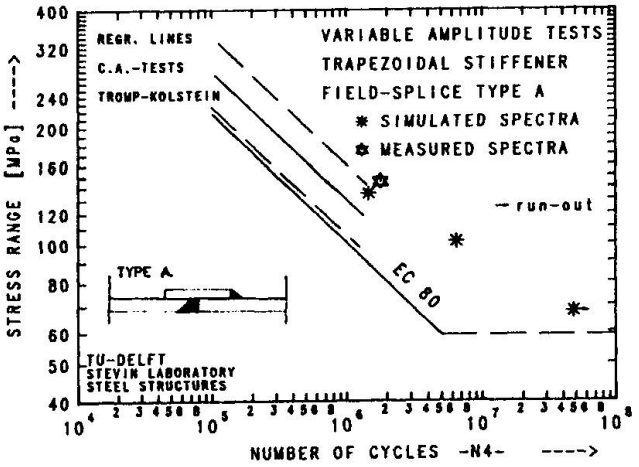

Test results Kolstein [Ref.4].
Figure 7.

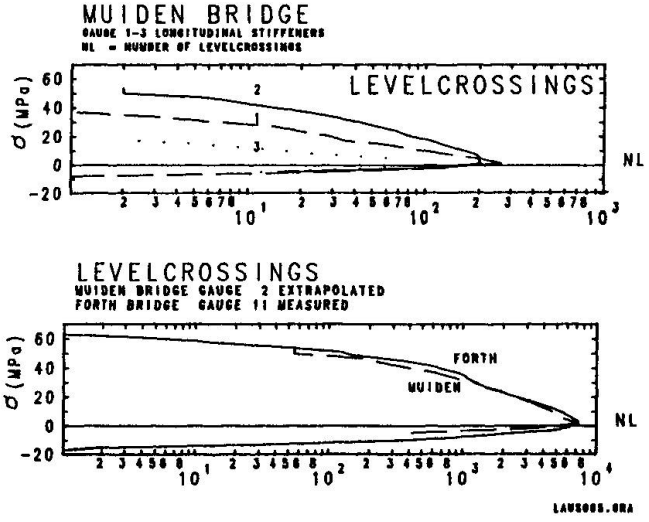

Measured stresses Muiden [Ref.8].
Figure 10.

for the design of new bridges [9]. Knowing the composition of a traffic, stress-time histories can be calculated by running that traffic over static influence lines.
Instead of the impact factor a so called fatigue-coefficient is used to represent the dynamic influence. It has been shown from measurements that the application of the usual impact factor led to results which are too pessimistic while the impact factor covers maximum values of the dynamic effect. In reality there is a scatter of stresses which have to be considered. A fatigue-coefficient being an average of the impact factor seems to be more realistic.
Using the rainflow counting method the stress-time histories are transformed into a number of stress cycles. After that the evaluated stress ranges of the different vehicles are expressed in a ratio to the the stress range $\Delta\sigma st$.
Doing this for several spans spectra of stress ranges can be composed for each span. To evaluate the fatigue life the cumulative damage hypothesis of Palgrem-Miner is applied, using the fatigue strength curves of the Eurocode.
Knowing the spectra with stress ranges expressed in a ratio to $\Delta\sigma st$, the fatigue life can be calculated for bridges of several spans and a chosen value $\Delta\sigma st$.
Figure provides the course of the procedure using an arbitrary S-N curve.
While all fatigue strength curves are similar, having the same slope and the kneepoint at the same number of cycles $N = 5.10^6$, a simplification in the calculations can be achieved by transforming the stress range $\Delta\sigma st$ into a dimensionless value, dividing $\Delta\sigma st$ by the value $\Delta\sigma$-2.10^6 of the considered S-N curve.
Now factors, k_1, applicable for all S-N curves can be evaluated to define the limiting stress range $\Delta\sigma st$ for an assumed life and the standard traffic.

$$\Delta\sigma_{st(lim)} = \frac{\Delta\sigma \; 2.10^6}{k_1 . \gamma}$$

Figure 11 shows the derivation and gives a set of factors k_1 for an assumed fatigue life of 50 years, respectively 100 years, for the mentioned standard traffic.

It can be concluded for a field splice in a longitudinal rib the static design stress range $\Delta\sigma_{st(lim)}$ with a cross-beam span of 4 meter and a weld class EC 80 must be $\leq$ 100 MPa. Considering the transverse distribution of the wheels and belonging influence line (fig.12) a fatigue reduction factor k_2 can be calculated by the following formula ;

$$k_2 = (\alpha_1 . \beta_1^m + \ldots\ldots + \alpha_i . \beta_i^m)^{1/m}, \text{ in which:}$$

α = transverse distribution factor of the wheel load
β = influence line factor for a specific point
m = slope of the S-N curve.

Now: $$\Delta\sigma_{st(lim)} = \frac{\Delta\sigma \; 2.10^6}{k_1 . k_2 . \gamma} .$$

For above mentioned situation $\Delta\sigma_{st(lim)}$ must be $\leq$ 140 MPa.

5. NEED FOR FURTHER WORK

It can be concluded, that the remaining fatigue life of the field- welded splices in longitudinal ribs in existing bridges will be very actual the following years. Therefore it is necessary to develop economic repairing techniques for these welded connections. Based on the available results on these detail, a better design can be realized for new bridges. However it is required to be very accurate concerning the quality of the welds.

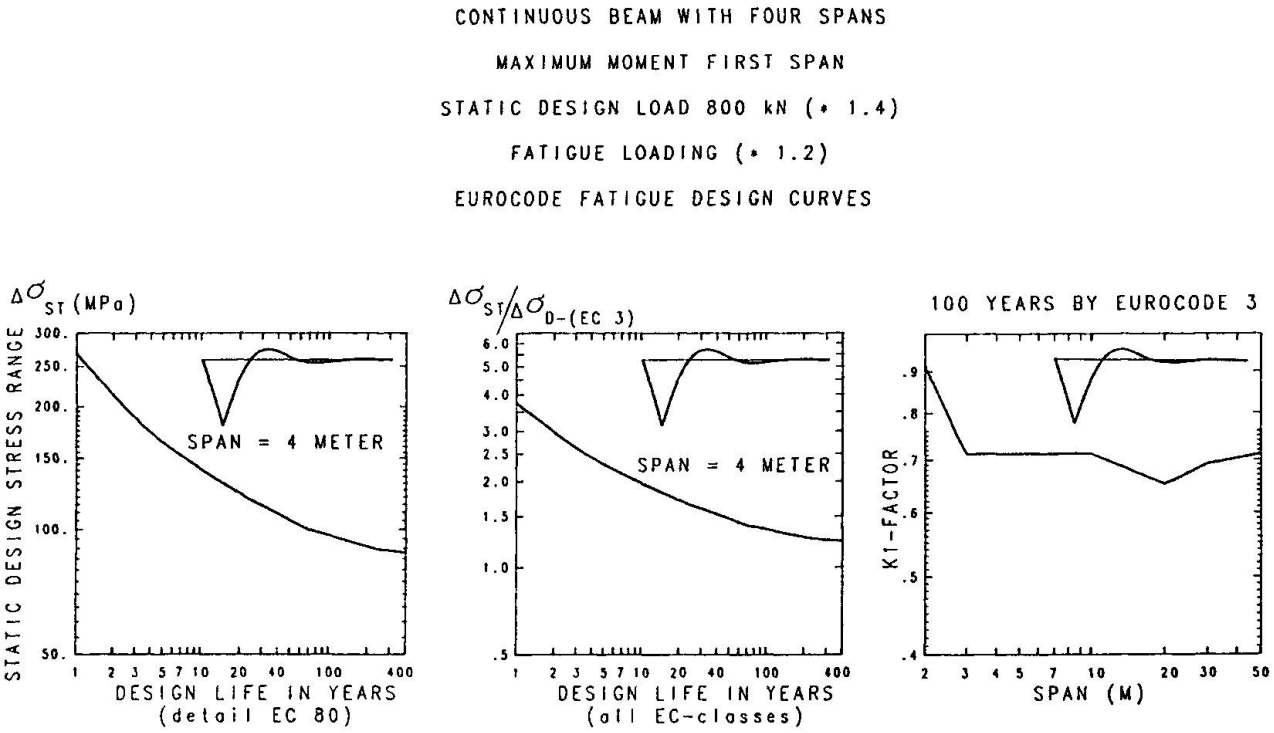

Fatigue design curves [Ref.9,10].
Figure 11.

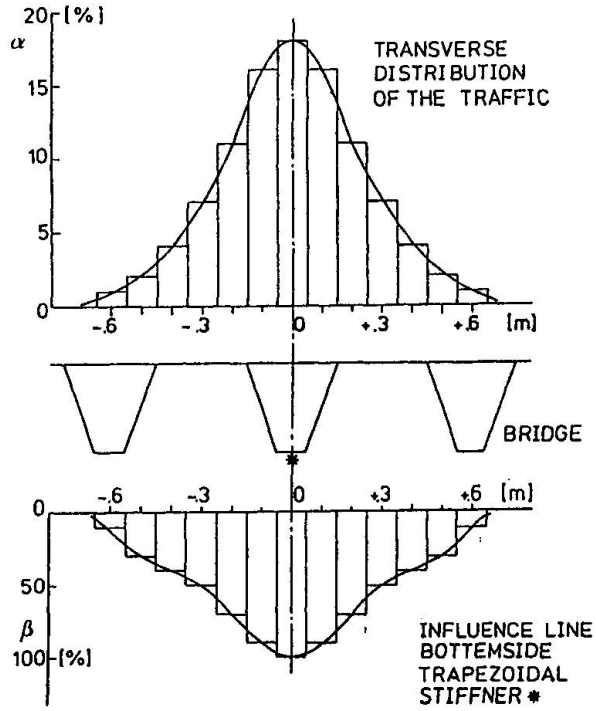

Transverse load distribution and influence line [Ref.10].
Figure 12.

6. ACKNOWLEDGMENTS

The authors wish to thank the colleagues in the European Working Group for their competent and stimulating discussions about the programmes and the results.
Some of the work described was carried out for the bridge department of the Dutch Governmental Organization 'Rijkswaterstaat'. Partial the published work was possible due to the financial aid of the Commission of the European Communities.
Moreover the authors wish to thank 'Rijkswaterstaat' and the Commission of the European Communities for their permission to publish this paper.

7. LITERATURE

1. TROMP W.A.J., Fatigue of field splices in ribs of orthotropic steel bridge decks. Stevinreport 6-74-15, Stevin Laboratory - Steelstructures Delft University of Technology, The Netherlands, 1974.

2. DE BACK J. BRULS A. CARRACILLI J. HOFFMANN E. SANPAOLESI L. TILLY J.P. ZASCHEL J.M., Measurements and Interpretation of dynamic Loads on Bridges, Synthesis Report - Phase 1, Commission of the European Communities, EUR 7754, 1982.

3. HAIBACH E. DE BACK J. BRULS A. CARRACILLI J. JACOB B. KOLSTEIN M.H. PAGE J. PFEIFER M.R. SANPAOLESI L. TILLY J.P. ZACHEL J.M. HOFFMAN E., Measurements and Interpretation of dynamic Loads on Bridges, Synthesis Report - Phase 2, Commission of the European Communities, EUR 9759, 1986.

4. KOLSTEIN M.H. DE BACK J., Fatigue strength of orthotropic steel decks; Part 1: Field-welded rib joints. ECSC Contract no. 7210-KD/609-F4.4/86. Stevinreport 25.6.89.30/A2, Stevin Laboratory - Steelstructures Delft University of Technology, The Netherlands, 1989.

5. YAMADA K. e.a., Fatigue Strength of Field-Welded Rib Joints of Orthotropic Steel Decks. IIW Doc. XIII-1282-88, Department of Civil Engineering, Nagoya University, Chikusaku, Nagoya 464, Japan, 1988.

6. SANPAOLESI L., Misure ed Interpretazioni dei Carichi dinamici sui Ponti Fase 3. Convenzione n° 7210-KD/411-F4.4/86. Instuto di Scienza della Costruzioni, Universita di Pisa, Italia, 1989.

7. CUNNINGHAME J.R., Fatigue performance of joints between longitudinal stiffeners. TRRL Laboratory Report 1066, Transport and Road Research Laboratory - Bridges Division, Crowthorne, United Kingdom, 1982.

8. KOLSTEIN M.H., Stuikverbindingen in trogvormige langsverstijvingen in een orthotrope rijvloer van een stalen verkeersbrug. Stevinreport 6-85-5, Stevin Laboratory - Steelstructures, Delft University of Technology, The Netherlands, 1986.

9. VAN MAARSCHALKERWAART H.M.C.M., Evaluation of existing structures. Proceedings of Fatigue aspects in structural design, Delft, The netherlands, 1989.

10. KOLSTEIN M.H., Presentatiewijze voor het op vermoeiing bereken van stalen verkeersbruggen. Stevinreport 6-85-17, Stevin Laboratory - Steelstructures, Delft University of Thechnology, The Netherlands, 1985.

Fatigue Tests of Stiffener to Cross Beam Connections

Essais de fatigue de liaisons entre raidisseur et entretoise

Versuche zur Ermüdung des Anschlusses einer Steife an einen Querträger

Hans-Peter LEHRKE
Dr.-Ing.
Frauenhofer-Inst. für Betriebsfestigkeit
Darmstadt, Fed. Rep. of Germany

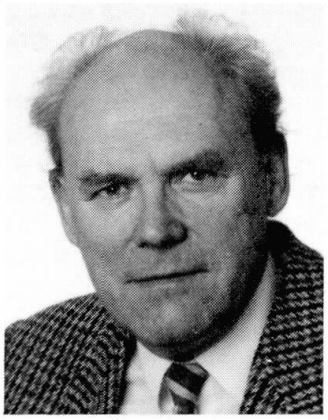

H.-P. Lehrke, born 1936, received his civil engineering and doctoral degrees at the Technical University, Braunschweig. After employment as an assistant at the Technical University, he was involved in mechanical and mathematical engineering problems at Krupp-Forschungsinstitut, Essen. Since 1973 he has been senior research engineer at LBF (Frauenhofer-Institut für Betriebsfestigkeit). Main research topics are fatigue, stress analysis, and dynamics of structures.

SUMMARY

Traffic loads produce high stress concentrations leading to fatigue cracking at the edges of cut-outs in webs of cross beams. High local stresses can be reduced by improved shaping of cut-outs. Fatigue tests were performed using two types of specimens; one with a commonly used shape of cut-out and the other with a new shape. The results showed a considerable increase of fatigue life for the new shape. However residual stresses of unknown distribution and high intensities were observed in all specimens and these may have influenced the increase in fatigue strength.

RÉSUMÉ

Les charges du trafic produisent des concentrations de contraintes élevées aux bord des découpes dans les âmes des entretoises pouvant conduire à un dommage en fatigue. Ces pointes de contraintes peuvent être réduites par des géométries de découpes plus favorables. Des essais de fatigue ont été réalisés sur des entretoises comprenant l'ancienne et la nouvelle géométrie. Bien que les résultats montrent un accroissement considérable de la durée de vie pour la nouvelle découpe, ceux-ci demandent encore à être confirmés du fait de la présence dans les éprouvettes de contraintes résiduelles inconnues et élevées qui peuvent avoir influencé cette amélioration.

ZUSAMMENFASSUNG

Verkehrslasten rufen an den Rändern der Ausnehmungen in den Stegblechen von Brückenquerträgern hohe Spannungsspitzen und möglicherweise Ermüdungsschäden hervor. Diese Kerbspannungen können durch eine günstigere Ausnehmungsform reduziert werden. Ausgeführt wurden Ermüdungsfestigkeitsversuche an Querträgern mit einer derzeit gebräuchlichen und einer neuen Ausnehmungsform. Die bisher erzielten Ergebnisse ergaben eine deutliche Lebensdauersteigerung für die neue Form, können aber nicht als abgesichert gelten, weil unbekannte Eigenspannungen hoher Intensität in sämtlichen Versuchsträgern beobachtet wurden.

1. INTRODUCTION

During the last years institutes from six European countries have performed a joint research program on steel bridges supported by the EC with the following main topics

- measurement and description of traffic loads
- operational stresses in steel bridge components and
- fatigue of orthotropic steel bridge decks.

The longitudinal stiffener to cross beam connection is one design detail of orthotropic decks susceptible to fatigue failure.

In orthotropic steel decks the traffic loads are transferred from the deckplate via the longitudinal stiffeners to the cross beams and from there to the main structure of the bridge. Depending on the number of traffic lanes, one cross beam may gather the loads of several wheels and axles belonging to more than one vehicle. Cross beams have the dimensions of beams. They are stressed by bending moments, shear forces and torsional moments. Besides the globally distributed beam stresses, additional stress fields are distributed more locally e.g. due to the load introduction and due to local stress concentrations.

Orthotropic decks in modern design contain cut-outs in the web of the cross beams to let the longitudinal stiffeners pass through. The cut-outs interrupt the stress fields and evoke stress concentration at their free edges. Besides the highly stressed edges, the welds connecting the stiffeners to the webs of the cross beams must also be regarded to be potentially critical to fatigue failure.

Approaching the real stress state in a bridge, two main load cases may be defined stressing the longitudinal stiffener to cross beam connection at the two critical points just mentioned:

- the load introduction into the cross beam which is passing the welds connecting the stiffeners to the web and
- the load transfer in the cross beam from the points of load introduction to the main structure of the bridge.

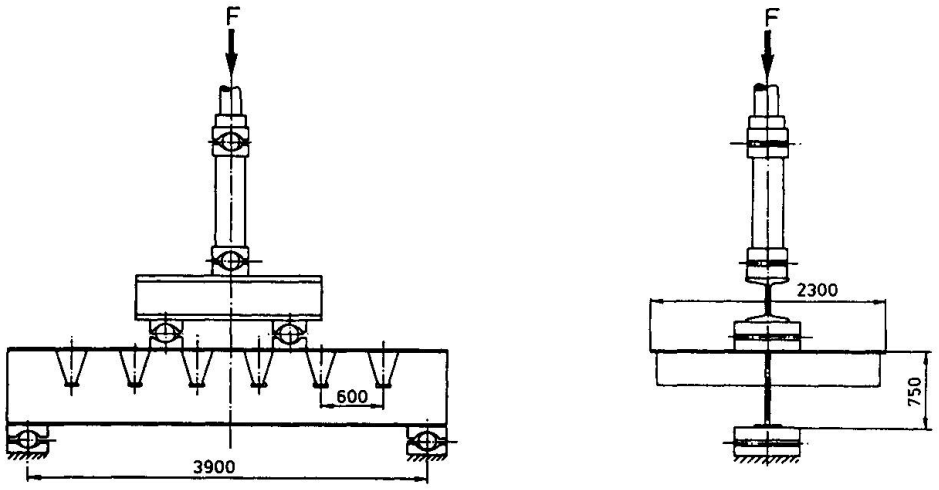

Fig. 1 Testing performed

Each load case may produce fatigue at both critical points. While the firstly mentioned load case is investigated by other groups in the joint research project, the objective of this paper is limited to the second load case. Thus, the function of cross beams to carry the loads of several wheels introduced at different points, as in large bridges with several traffic lanes, is emphasized.

2. STRESS ANALYSIS

A simply supported cross beam loaded by a shear force and a bending moment may be used as a model to simulate the load case of interest.

As a first approach to calculate the stress distribution in the critical regions, the web was modelled by two-dimensional in-plane finite elements, and the deck plate together with the stiffeners by in-plane beam elements of equivalent stiffness.

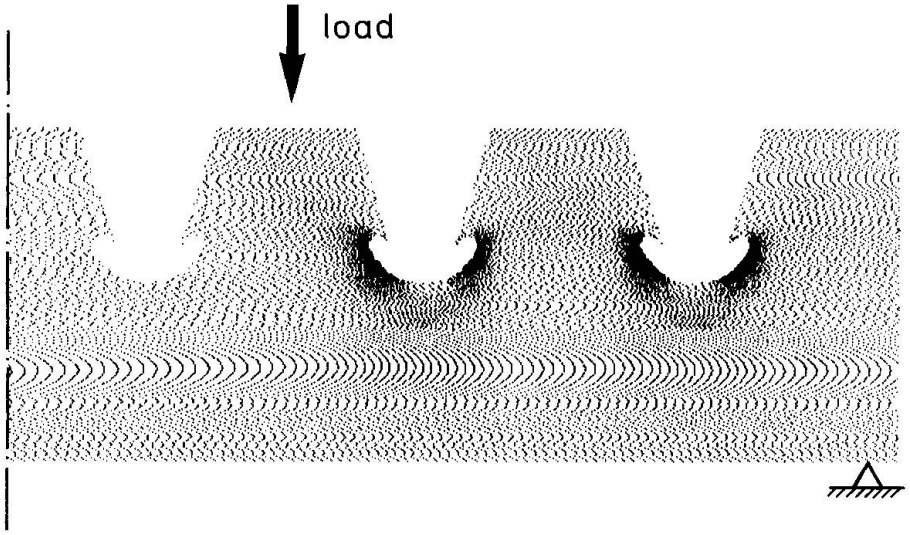

Fig. 2 Global stress distribution in one half of the web loaded as in Fig. 1

Fig. 2 gives an impression of the global stress distribution in the web of one half of the symmetrically loaded cross beam. High stress concentrations occur at the edges of the cut-outs but only in the beam segment loaded by a shear force. The level of high spot stresses depends on the shear force and nearly not on the bending moment. These high stresses at the edges of the cut-outs can be explained by bending the so-called teeth of the web located between each two cut-outs. The bending is produced by a shear force acting between each tooth and the deck plate because the deck plate is the upper flange of the cross beams.

Fig. 3 shows the distribution of the bending stresses in the narrowest section of one tooth between two cut-outs calculated by finite elements and verified by strain measurements. When comparing the highest spot stress with the nominal bending stress at the edge of the cut-outs, the stress concentration factor can be estimated. It yields $K_t \approx 2.8$ in this example.

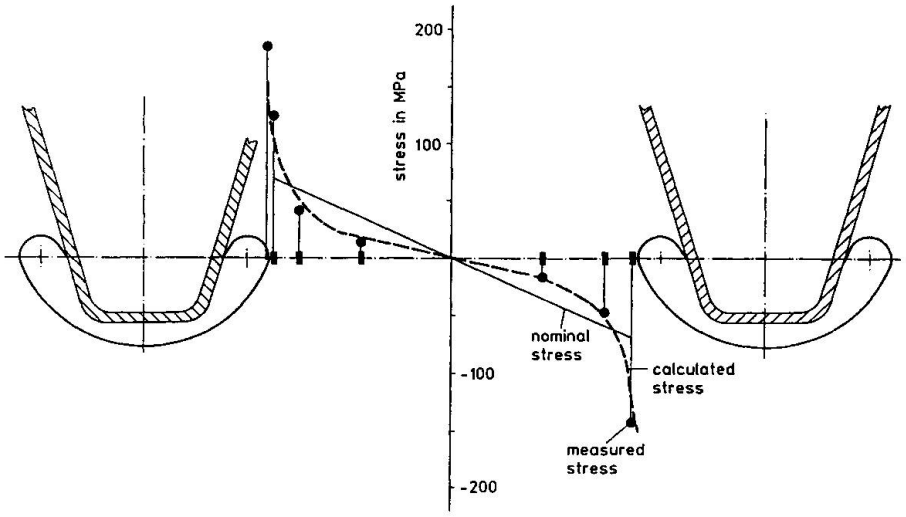

Fig. 3 Stress distribution in the narrowest section between two cut-outs

Generally, the stress level at the edges of the cut-outs exceeds the stresses in all other parts of the web by a factor larger than 5. Therefore, one design objective must be to have a better exploitation of material i.e. to reduce the stress concentration. Basically, this can be achieved by an extension of the distance between the stiffeners. This, however, requires a change of the whole orthotropic deck design. Therefore, the only reliable solution seems to be to change the cut-outs' shape. But this may influence fatigue at the second critical point where the welds connecting the stiffeners to the web meet the cut-outs.

After investigating cross beams of railway bridges, Haibach and Plasil proposed a new shape of cut-outs [1]. They found it superior with respect to fatigue to the commonly used shape when performing fatigue tests on cross beams simulating the particular load case of a railway bridge with one rail. But they did not quantify the gain with respect to strength and fatigue life. This question and the question whether the new shape can also be recommended for large highway bridges under the load case just defined are of interest.

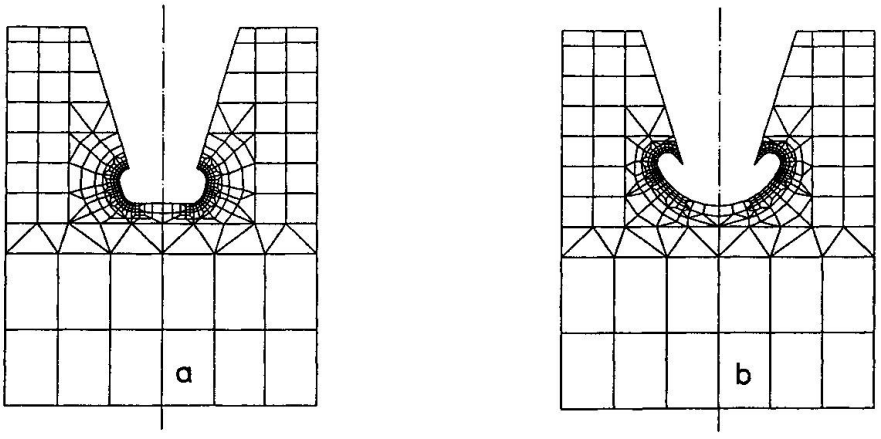

Fig. 4 Cut-outs of the commonly used (a) and of the new (b) shape modelled by finite elements

Fig. 4 shows the commonly used and the new shape of cut-outs modelled by finite elements. The stress distributions along the edges of both types of cut-outs differ significantly (Fig. 5) when the cross beam is loaded as shown in Fig. 1. But the levels of the maximum stresses are nearly the same. Only the volume of highly stressed material and the highly stressed surface at the edges of the cut-outs, respectively, are considerably larger for the commonly used shape. Besides this small advantage of the new shape at one of the critical points, the stresses are reduced at the second point where the welds meet the cut-outs. This result was verified by measurements because the accuracy of the used finite element model is questionable in the vicinity of the welds.

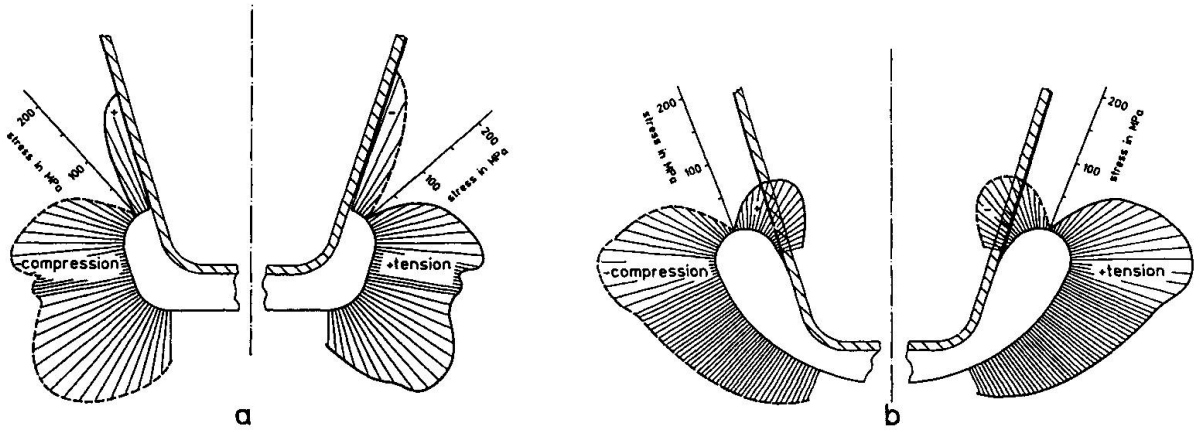

Fig. 5 Stress distribution along the edges of the cut-outs of the commonly used (a) and the new (b) shape

3. TEST DESCRIPTION

Three test specimens of nearly original size were fabricated as orthotropic decks of real bridges, each consisting of a cross beam, six stiffeners, and a deck plate made of structural steel St.53 (Fig. 1). The dimensions of all three specimens were identical except that one had cut-outs of the commonly used shape and the other two the proposedly improved shape. When a specimen is loaded as shown in Fig. 1, four of the six cut-outs are stressed nearly at the same level. This is due to the equal shear force at four of the cut-outs. Therefore, from each fatigue test up to four results could be expected, provided that cracks are detected early and repaired. Three fatigue tests were performed, one with constant amplitude loads applied to a specimen with cut-outs of the new shape and two using identical variable amplitude load sequences applied to the other two specimens with differently shaped cut-outs.

At the beginning of each test, the strains were measured at symmetrically located points on each specimen to guarantee the symmetry of loading. In particular, the torsional moment in the specimens was observed and reduced by changing the points of load introduction until its contribution to the maximum stresses was less than 5 %. Thus, reproducible test results could be expected.

The traffic induces mainly fluctuating compressive loads on the cross beams of bridges. The test rig with the simply supported cross beam allows to simulate this loading.

3.1 Constant amplitude test

The load range of the constant amplitude test was determined taking into account the test results of Haibach and Plasil [1] at

$\Delta P = 485$ kN
with an upper load of $P_u = 500$ kN
and a lower load of $P_l = 15$ kN.

This load results in a stress range of $\Delta \sigma = 480$ Mpa

at the edges of the cut-outs with
an upper stress of $\sigma_u = 495$ Mpa
and a lower stress of $\sigma_l = 15$ Mpa.

The results of the constant amplitude test are given in Fig. 6.

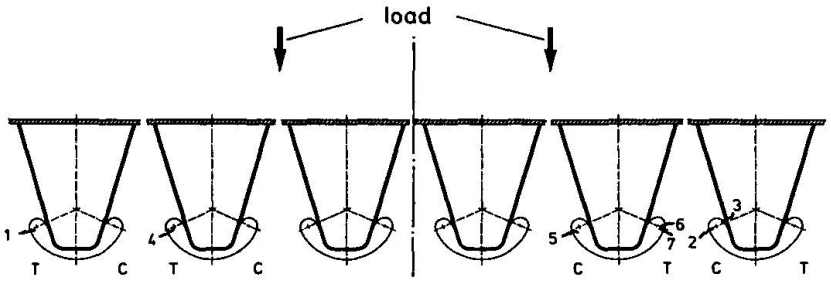

T: region with tension stresses
C: region with compression stresses

crack no. 1 after 205 000 cycles
crack no. 2 after 339 000 cycles
crack no. 3 after 339 000 cycles (no crack growth observed)
crack no. 4 after 344 000 cycles
crack no. 5 after 350 000 cycles
crack no. 6 after 350 000 cycles
crack no. 7 after 350 000 cycles

Fig. 6 Results of the constant amplitude test on one of the specimens with cut-outs of the new shape

3.2 Variable amplitude tests

Time histories of traffic loads acting on bridge components may be found by measurements or may be derived by a computer program developed as a part of the joint research project [2]. The program requires input data to describe the traffic on the bridge and the load transfer in the bridge from the wheel contact points to the points of interest. Fig. 9 shows a frequency distribution of range pair cycles counted from a load time history of a cross beam, which was calculated by the program due to 10000 vehicles passing the bridge on one lane.

From this range pair frequency distribution a first load sequence to be applied to the tests was developed by randomly deriving compressive load cycles. Although the initially calculated load time history contains small traction forces besides high compressive forces due to the applied influence line of load transfer, the load sequence used only compressive load cycles to maintain the simple test rig of Fig. 1.

As a result of damage calculation by Miner's Rule and in order to achieve acceptable test times an omission level was chosen that reduced the applied frequency distribution of Fig. 7 to 3084 from originally 15243 cycles which produce 98.5 % of the calculated damage. The load level was fixed to

the maximum load	P_{max}	=	500 kN
the minimum load	P_{min}	=	15 kN and
the maximum load range	ΔP_{max}	=	485 kN

which means the same nominal loads as in the constant amplitude test.

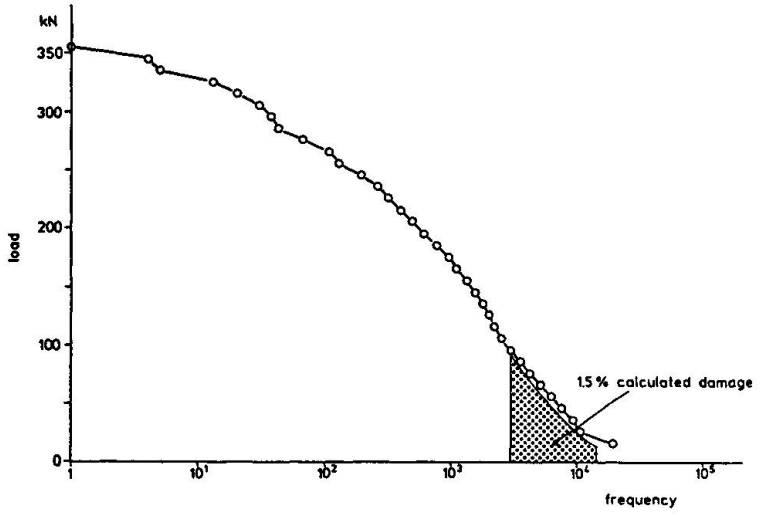

Fig. 7 Frequency distribution of the load sequence used in the variable amplitude tests

The results of both variable amplitude tests with the specimens of both cut-out types are given in Fig. 8 and 9.

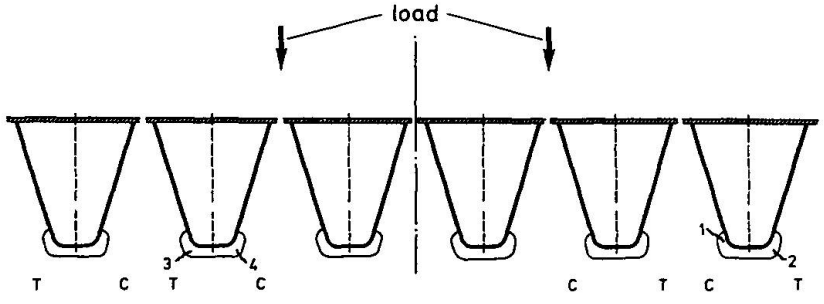

crack no. 1 after 2 844 200 cycles
crack no. 2 after 3 409 900 cycles
crack no. 3 after 4 541 000 cycles
crack no. 4 after 5 780 300 cycles
end of test after 5 926 600 cycles

Fig. 8 Results of the variable amplitude test on the specimen with the commonly used shape of cut-outs

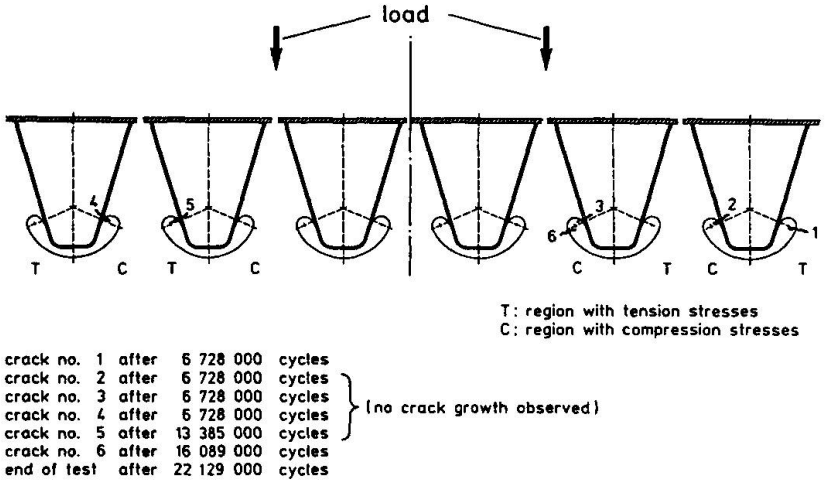

Fig. 9 Results of the variable amplitude test on one of the specimens with cut-outs of the new shape

4. DISCUSSION OF TEST RESULTS

Cracks were observed at both critical points of the stiffener to cross beam connection. Cracks at the ends of the welds occured only in the specimens with the new shape of cut-outs, although this shape was developed to reduce the stresses in this region. In fact, the stresses due to the external loads are really low, as proved by measurements. Therefore and since the cracks did not grow after their detection, residual stresses must have contributed to crack initiation.The new shape of the cut-outs seems to favour residual stresses to appear locally at the ends of the welds because the heat-flux into the web is during the welding restricted by the small area of material.

In contrast, the cracks initiated at the free edges of the cut-outs grew and would have destroyed the specimens if they had not been repaired. These cracks occurred at the cut-outs of the new shape after a 3 - 5 times higher number of load cycles than at the commonly used shape during the identical variable amplitude tests This is a considerable improvement of fatigue life.

However, cracks occurred at edges stressed in compression under external loads while other edges stressed in tension at the same level remained crack-free. The cracks under tension grew faster than those under compression. Moreover, the cracks in the compression regions remained open when the load was removed. These observations can only be explained by residual stresses globally distributed in all three specimens.

Residual stress fields are known to exist in large welded structures. Thus it is not clear, whether the observed increase of fatigue life can be attributed to the new shape of the cut-outs or is at least partially due to a more favourable residual stress distribution. These doubts are supported by the results of stress analysis which show no significant differences between the maximum stresses at both types of cut-outs (Fig. 5).

All test results are summarized in Fig. 10, those of the variable amplitude test on the specimen with cut-outs of the new shape in two representations one using nominal loads and really endured load cycles and the second using equivalent loads and equivalent load cycles as defined in Fig. 10. This was done to compare all results from the specimens with the new shape of cut-outs and to estimate their S-N-curve.

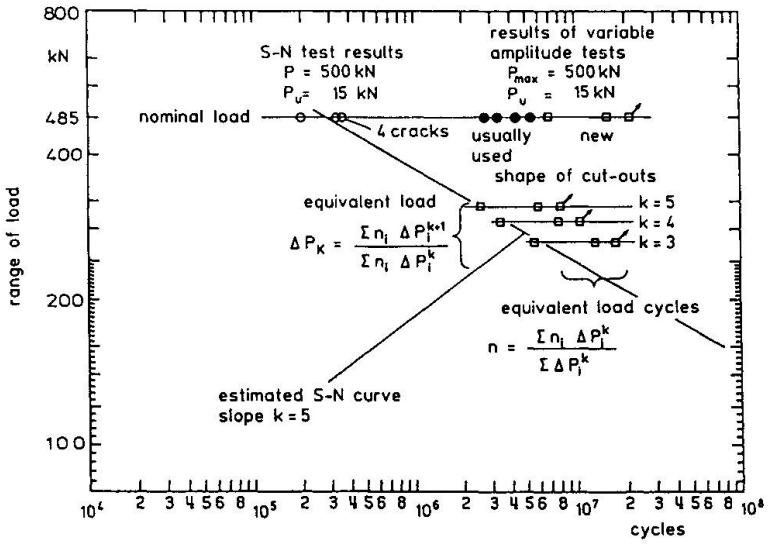

Fig. 10 All results of three tests

5 CONCLUSIONS

As a consequence of the above-mentioned shortcomings a recommendation for the new shape is not yet possible, though it showed an improved fatigue behaviour in the test performed. The following measures during design and fabrication can improve the fatigue strength at both mentioned critical points of the stiffener to cross beam connection

- a reduction of the stress concentration at the edges of the cut-outs by increasing the notch radius
- a reduction of the residual stresses at the ends of the welds between the stiffeners and the web by a shape which improves the heat-flux during welding
- the control of residual stresses introduced into the structure during fabrication to avoid unfavourable residual stresses.

REFERENCES

1. HAIBACH E., PLASIL I., Untersuchungen zur Betriebsfestigkeit von Stahlleichtfahrbahnen mit Trapezhohlsteifen im Eisenbahnbrückenbau. Der Stahlbau 9, 1983.

2. BRULS A., Mesures et Interpretation des Charges Dynamiques les Ponts. Rapport Final de la Premier Phase de la Research. Liège, 1979.

Leere Seite
Blank page
Page vide

Assessment of Fatigue Life of Orthotropic Steel Decks

Evaluation de la durée de vie des dalles orthotropes en acier

Berechnung der Lebensdauer orthotroper Platten aus Stahl

Aloïs BRULS
Lecturer
University of Liège
Liège, Belgium

Aloïs Bruls, born 1941, received his civil engineering degree from the University of Liège in 1965. He is currently a research engineer with the laboratory of the Department of Bridge and Structural Engineering at the University of Liège and a consultant with the company Delta G.C. in Liège.

SUMMARY

Using traffic measurements, a finite band computer program calculates stress range histograms at the joints where cracks occur. Further, as the fatigue strength has been obtained by tests, the fatigue life is calculated. Finally general information is given that allows an orthotropic steel deck design to account for traffic flow.

RÉSUMÉ

En considérant des mesures du trafic, un programme d'ordinateur utilisant les bandes finies calcule les histogrammes des amplitudes de contraintes aux points d'apparition des fissures. Par ailleurs, comme la résistance à la fatigue a été obtenue sur la base d'essais, la durée de vie est calculée. Finalement, des informations générales sont données pour la conception des dalles orthotropes en acier en fonction du volume de trafic.

ZUSAMMENFASSUNG

Mit Hilfe eines Finite-Elemente-Programmes werden unter Berücksichtigung von Verkehrsmessungen für Punkte, von denen Risse ausgehen, Histogramme der Spannungsamplituden berechnet. Da die Ermüdungsfestigkeit aus Versuchen bekannt ist, kann die Lebensdauer berechnet werden. Es folgen einige allgemeine Angaben zum Entwurf orthotroper Stahlfahrbahnplatten in Abhängigkeit des Verkehrsvolumens.

1. INTRODUCTION

The main parts of the connection stiffener-deck are the deck plate, the stiffener and the weld between them.
Usually the deck plate is minimum 10 or 12 mm thick and the surfacing thickness is, following the case +/- 10 mm or +/- 60 mm.

The stiffener studied have a closed trapezoïdal shape (Fig. 1). Stiffener dimensions are about 300 mm wide, 250 mm high and 6 mm thick. They are placed 300 mm apart. Because of the closed sections of stiffeners, welding is realized on only one side of the stiffener web. The aim of this work is to know the fatigue life of this weld. Therefore, we use wheel load measurements of traffics, a finite band computer program and fatigue tests. This paper summarizes a work realized in Belgium with the help of the European Community [1].

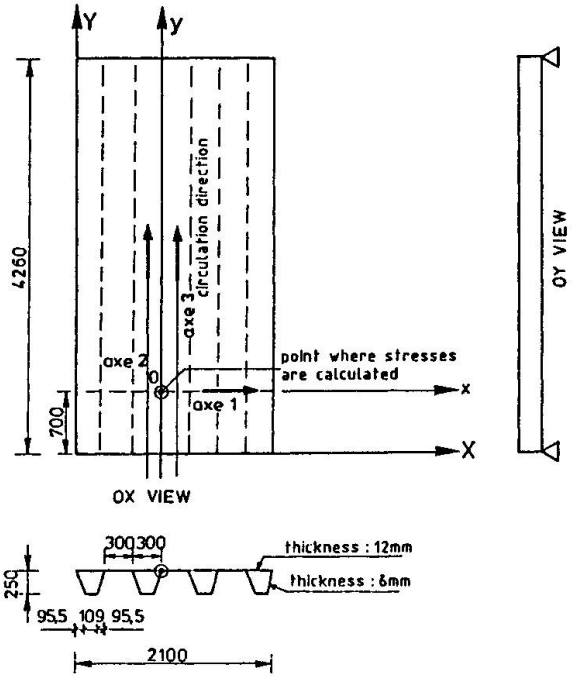

Fig.1 : Structure used for the calculation

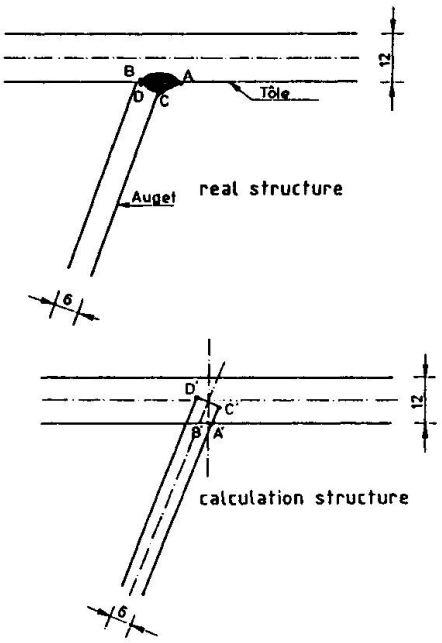

Fig. 2 : Detail

2. STRESS DETERMINATION

2.1 Traffic measurments

During previous works [2][3], the stresses near the weld are measured under traffic loads and under vehicles of calibrated load. These measurements are influenced by the distribution of wheel load, in intensity, in transverse position, and by temperature. The temperature influences the behaviour of the surfacing and its collaboration with the steel plate. On the other side, it is not possible to measure a stress at crack initiation point.
As simultaneously with the stress measurements, the axle loads of the vehicles are recorded, load histograms may be established for three types of wheels : normal wheel, extra large wheel, twin-wheels.

In this paper we consider only the traffic recorded in Rheden in 1978, because it is very well known and very aggressive [4].

2.2. Calculation

In view to have a general approach of the behaviour of the weld connection under wheel load, it is necessary to develop a stress calculation method. Stresses have been calculated by a finite band program. The frame used for the calculation has the geometry of orthotropic decks met in Belgium bridges (Fig. 1). The points where stresses are calculated are located in the neighbourhood of the weld (Fig. 2). Points A', B' : in the deck plate ; points C', D' : in the weld.

Axial and bending stresses are calculated in the cross-section in which they are the highest (section 0 - axis 1 - Fig. 1).
With the finite band program it is possible to study influences of the following parameters :

- dimensions of wheel contact area depending of the type of wheel (Fig. 3) and the surfacing :
  - deck without surfacing :load does not diffuse ;
  - deck with a 60 mm surfacing thickness : load diffuses through the tickness with an angle of 45° ; no composite effect is considered.

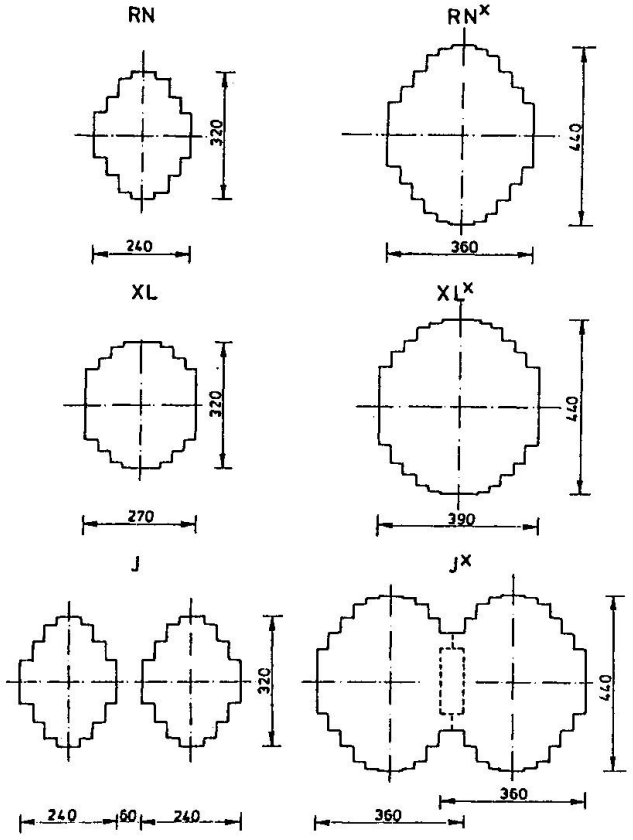

Fig 3 Wheel contact area

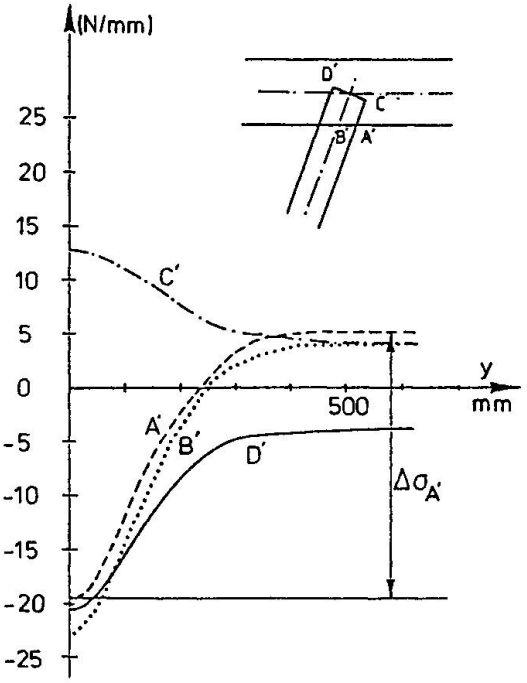

Fig. 4 σ influence line in 0 for a 10kN circulating on axis 2

- wheel longitudinal location : longitudinal influence lines are drawn in Fig. 4. It appears that at points A' and B' (deck plate) stress values change sign at a certain distance from 0 section. Thus stress amplitude at point A' and B' is higher than the maximum stress obtained when the wheel is on axis 1 ;
- wheel transverse location : results are presented in forms of transverse infuence lines (Fig. 5 and 6).

2.3. Stress histograms.

The calculation of the stress spectra is made by means of the simulation program [5][6]. For each axle of the traffic the program chooses at random a transverse position on the deck plate to which corresponds a value of the transverse influence line (Fig. 5 and 6). This value, multiplied by the load of the axle, gives the stress induced.

The data introduced in the simulation program are :

1. Traffic : the vehicle axles of the Rheden traffic have been divided in four groups according to their wheel type [4].
2. Transverse distribution : the axle transverse distribution is obtained from measurements [2][3].
3. Transverse influence lines : calculated following the above mentioned computer program.

The histogram obtained at point D' and given in the table 1 is used for fatigue tests under variable amplitude and for the fatigue life calculation.

Stresses σ_i (N/mm²)	Number	Stress-ranges $\Delta\sigma_i$ (N/mm²)	Number
70 - 80	13	10 - 20	6767
60 - 70	19	20 - 30	4163
50 - 60	61	30 - 40	2489
40 - 50	222	40 - 50	1690
30 - 40	635	50 - 60	1090
20 - 30	1175	60 - 70	872
10 - 20	2751	70 - 80	601
0 - 10	5176	80 - 90	441
0	12627	90 - 100	314
-10 / -0		100 - 110	253
-20 / -10	6629	110 - 120	142
-30 / -20	4348	120 - 130	134
-40 / -30	2348	130 - 140	81
-50 / -40	1668	140 - 150	48
-60 / -50	1068	150 - 160	17
-70 / -60	570	160 - 170	21
-80 / -70	365	170 - 180	11
-90 / -80	189	180 - 190	7
-100 / -90	83	190 - 200	5
-110 / -100	36	200 - 210	2
-120 / -110	9	210 - 220	2
-130 / -120	7		
-140 / -130	2		
TOTAL	40000	-	19150

Table 1

Stress and stress-range histograms at point D' (variable amplitude tests)

Fig 5 : σ_A Influence lines for a wheel (axis1 ; y=0) transverse repartition

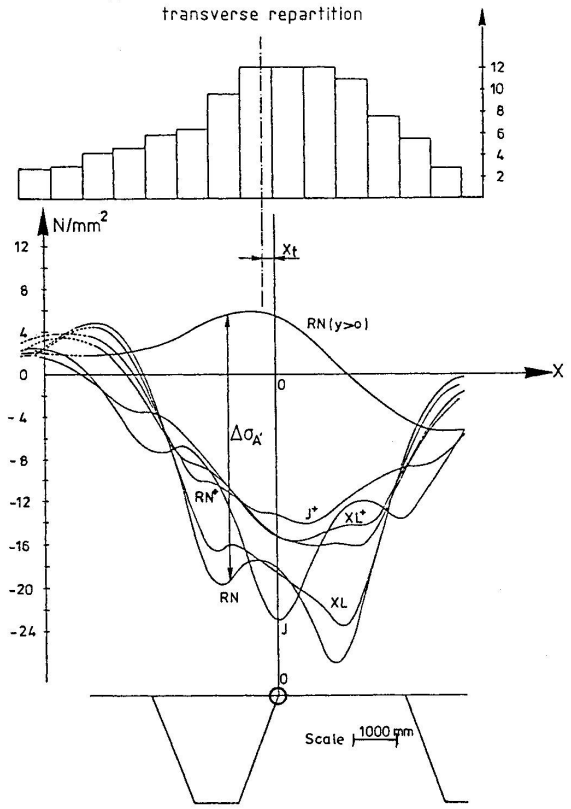

Fig 6 : σ_D Influence lines for a wheel (axis1 ; y=0) transverse repartition

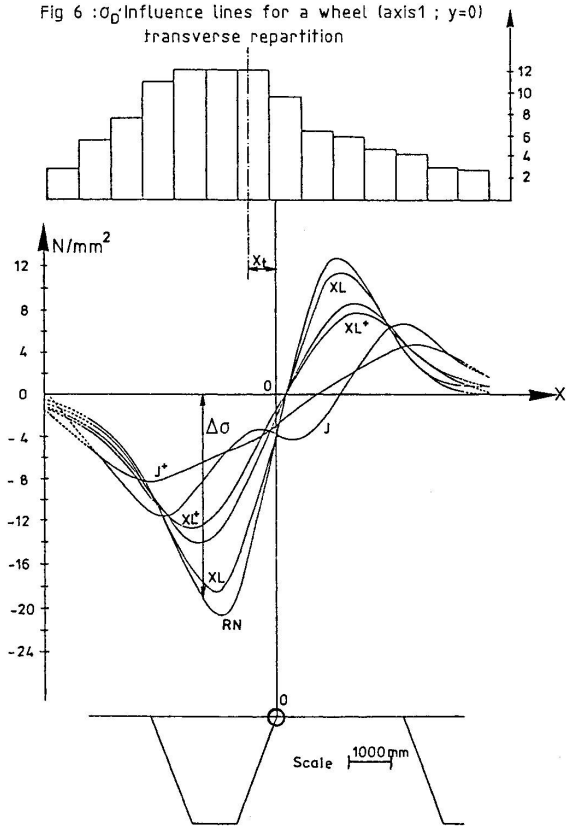

3. FATIGUE STRENGTH

3.1 Test specimens

The loading mode and the geometrical characteristics of the specimens are given in figure 7.
The material used is of the type E 36-4.
General welding procedure characteristics are :

- no edge stiffener preparation ;
- horizontal position ;
- one run ;
- no preheating ;
- no postheating ;
- automatic welding (submerged arc).

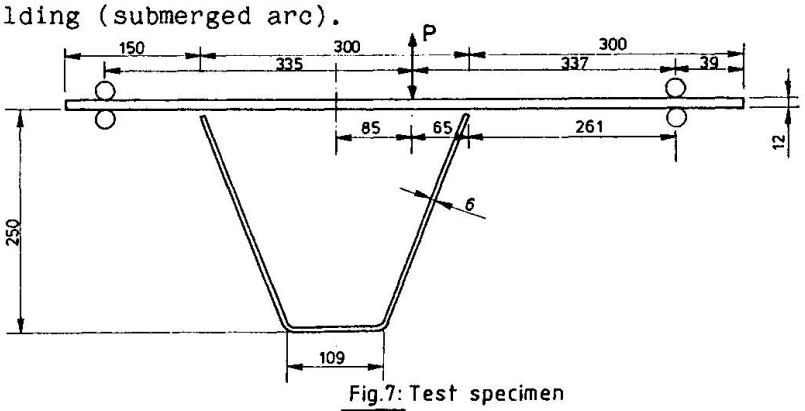

Fig.7: Test specimen

Welding procedure has evolved : firstly the procedure was manual (CRIF [7]), now it is automatic submerged arc welding and it is still evolving to obtain a smaller lack of penetration.

The geometrical characteristics of the welds tested are given in table 2.

Specimen	Lack of penetration	Fillet weld
CRIF [7]	3,0 to 4,5 mm	3,5 to 4,5 mm
Ulg [1]	1,5 to 2,5 mm	4,7 to 6 mm
IRSID [8]	+/- 1 mm	5,5 to 6,5 mm

Table 2

The tests realized under constant amplitude determine the S-N curve. Some tests realized under variable amplitude gives information about the possibilities of a damage calculation applicating the Miner Rule.

3.2. Test result

3.2.1. Presentation

Depending on the stress distribution in the deck plate and in the trough, as well as the weld quality (penetration, throat, underents, ...,) fatigue cracking may occur either :

a) from the weld toe on the deck plate, point A Fig. 2, and develops in the decks plate that corresponds to $\Delta\sigma_d$;

b) from the weld root in the stiffener, point D Fig. 2, and develops in the throat of the weld ; that corresponds to $\Delta\sigma_s$.

From these tests are derived the nominal stresses definition to be used in the fatigue S-N diagrams, by extrapolating the measured stresses.
The results obtained earlier by CRIF [7] and recently by ULg [1] and IRSID [8] are presented on Fig. 8 and Fig.9.

3.2.2. Failure in the deck plate $\Delta\sigma_d$.

Tests under constant amplitude determine the fatigue strength of the deck plate at the weld toe. Results are plotted on Fig. 8.

Main conclusions are :

- There is no significative differences between specimen with 2 mm gap between the top of the stiffener web and the deck plate and specimen with no gap provided the lack of penetration is less the 2 mm.
  The mean Wöhler curve is determined with $R_S = 1$ in the weld root for the specimen tested at IRSID :

$$\Delta\sigma_d = 26777\ N^{1/3} \quad (m = 3 \text{ imposed})$$

  and the characteristic value for 97,5 % is

$$\Delta\sigma_{dc} = 163\ N/mm^2 \text{ for } N_c = 2.10^6 \text{ cycles.}$$

- The two tests conducted at IRSID show a lower fatigue resistance at R = 0,1 than R = -1. Nevertheless, two similar tests performed at Liège do not indicate such a detrimental effect.
  In only two U.Lg. specimens did failure occur in the deck plate that corresponding to $R_S = 0$ (only tensile at point A).

The loading histogram used for tests under variable amplitude is the stress spectra calculated (table 1). This histogram simulates traffic effects. Loads are applied at random on the test specimen, taking in account the sign of the stresses. The results of tests are plotted in Fig. 8 by their equivalent values $\Delta\sigma_e$, n_e calculated from the histogram with an SN curve with a slope of -1/3, corresponds to the centre of gravity of the damage distribution [9][10] :

$$\Delta\sigma_e = \frac{\sum_{\Delta\sigma_i}^{\infty} n_i . \Delta\sigma_i^4}{\sum_{\Delta\sigma_i = 0}^{\infty} n_i . \Delta\sigma_i^3} \qquad n_e = \frac{\sum_{\sigma_{i=0}}^{\infty} n_i . \Delta\sigma_i^3}{\Delta\sigma_e^3}$$

Results are similar to those obtained with constant amplitude loading.

3.3.3. Failure in the weld $\Delta\sigma_s$.

Tests results under constant amplitude are plotted on Fig. 9.
Main conclusions are :

- the fatigue strength increases significantly when using automatic welding, this technique allows larger penetration and throat thickness at the weld.
- the mean S-N curve is determined for automatic welding :

$$\Delta\sigma = 17258\ N^{1/3}$$

and the characteristic value for 97,5 % is

$\Delta\sigma_{sc}$ = 114 N/mm² for $N_c = 2.10^6$ cycles.

- The tests show the importance of R_s ratio. To obtained the failure in the weld it was necessary to have more tension than compression at the root of the weld (point D) :

$1 < R_s < 0$ in the Ulg specimens

R_s = 0,1 in the IRSID specimen.

The loading histogram used for tests under variable amplitude is the calculated stress spectra (table 1).
The loads are applied random, but to obtain failure in the weld (point D), it has been necessary to change the sign of the stress calculated, so that there is more tension than compression : R_s = -0,5 instead of - 2,0 at the root for the highest stress range.
The results are plotted in Fig. 9 by their equivalent values assessed as in Fig. 8.
Results are similar to those obtained with constant amplitude loading.

4. FATIGUE LIFE CALCULATION

We consider as characteristic stress range the values deduced from the fatigue tests. For $N_c = 10^6$ cycles :

$\Delta\sigma_{sc}$ = 114 N/mm² , if the crack occurs in the weld (point D) ;

$\Delta\sigma_{dc}$ = 163 N/mm² if the crack occurs in the plate (pointe A).

Following Eurocode 3, the SN curves have two slopes : m = 3 for $N < 5.10^6$ and m = 5 for $5.10^6 < N < 10^8$.
If the traffic composition measured in Rheden is considered [4], the allowed number of lorries during the life time may be calculated. The results are given on table 3.
Putting there data in perspective the traffic flows recorded on highways generally comprise between 1000 and 4000 lorries during a working day [2][3]. Such flows produce after 100 years between 20 and 80.10^6 lorries.
The examination of table 3 calls the following comments :

1. The fatigue life calculated in the deck ($\Delta\sigma_d$) is always a little longer than in the weld ($\Delta\sigma_s$) : the higher strength is partially offset by higher stress ranges produced in this point by the traffic loads ;

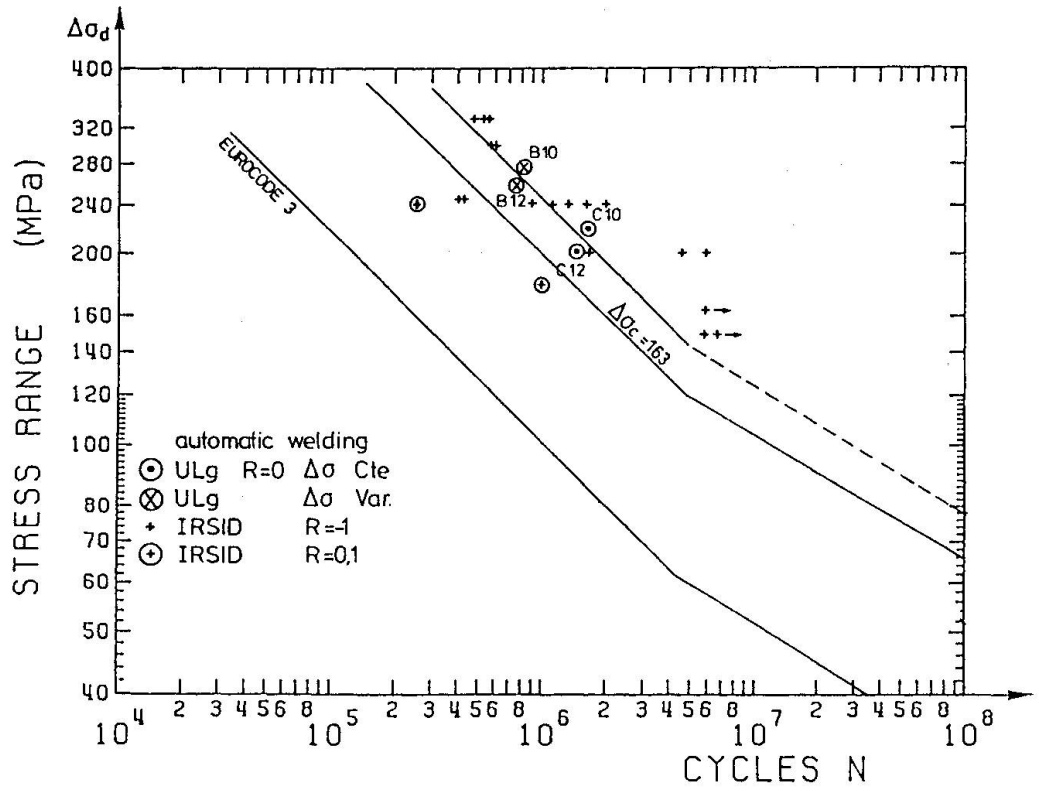

Fig.8: Crack initiation at the weld toe : $\Delta\sigma_d$

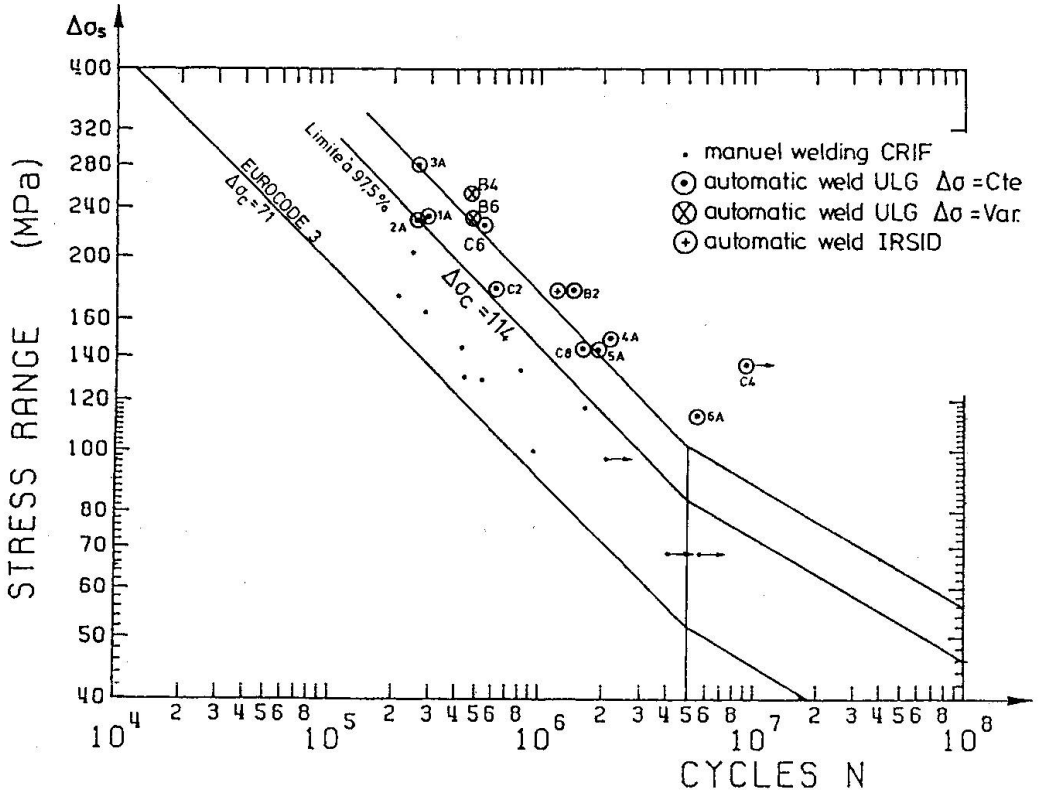

Fig.9: Crack initiation at the weld root: $\Delta\sigma_s$

Fatigue life

Connection Stiffener - Deck plate

Thickness (mm)			Number of lorries (10^6)	
Plate	Stiffener	surfacing	$\Delta\sigma_s$	$\Delta\sigma_d$
12	6	0	20	20
12	6	60	71	75
13	6	0	44	45
13	6	60	199	219
14	6	0	89	103
14	6	60	494	647
14	7	0	62	73
14	7	60	297	393

Table 3

2. A surfacing of 60 mm gives a fatigue life 3 to 5 times longer, than the unsurfaced deck ;

3. An increase in the plate thickness of 1 mm gives a fatigue life +/-2 times longer.

4. An increase in the thickness of the stiffener reduces the fatigue life a little.

5. The given fatigue lives are pessimistic, because the transverse position of the traffic flow considered in the calculation is the most unfavourable and in surfaced deks, now composite effect is considered.

We may conclude :

1° For the weld tested, the failure may not occur in the weld but in the plate, if the thickness of the plate is at least twice as thick as that of the stiffener ;

2° the required thickness of the deckplate depends on the expected number of lorries and the thickness of the surfacing.

5. CONCLUSIONS

The specimens used in the experiments were welded with automatic submerged arc welding in an industrial situation. It has been shown that full penetration, (lack of penetration lower than 1 mm.) can nearly be achieved without edge preparation.

In these conditions, there is no significant difference in fatigue behaviour for specimens with a 2 mm gap by welding or without gap.

For alternate bending, that is a little more severe than the loading in bridges, with a lack of penetration not greater than 1 mm, the cracks initiate at the weld toe in the deck plate.

Using a computer band program it is possible to calculate the fatigue life of the connection taking in account :

- thickness of the surfacing that increases the wheel contact area ;
- geometry of the orthotropic deck ;
- traffic defined by a number of lorries and by load histograms for each type of wheel.

To increase the fatigue life, the designer has the possibility to choose between increasing the thickness of the surfacing or that of the steel plate. Table 3 gives fatigue lives for common sizes of orthotropic plate (Fig. 1).

REFERENCES

[1] BRULS A., POLEUR E. Mesures et interprétation des charges dynamiques dans les ponts - 3e phase - Resistance à la fatigue des dalles orthotropes. Recherche CECA-1989.

[2] De BACK, BRULS, CARRACILLI, HOFFMAN, SANPAOLESI, TILLY, ZASCHEL. Mesures et interprétation des charges dynamiques dans les ponts. Rapport commun de synthèse - 1ère phase - Recherche CECA. Rapport EUR. 7754.1982.

[3] HAIBACH, BRULS, de BACK, CARRACILLI, JACOB, KOLSTEIN, PAGE, PFERFER, SANPAOLESI, TILLY, ZASCHEL. Measurements and interpretation of dynamics loads on bridges - Synthesis report of the 2nd phase - ECSC Research - Rapport EUR 9759. 1986.

[4] De BACK, KOLSTEIN, Measurements and interpretation of dynamics loads on briges. 2d phase. ECSC Research - Report 6.83-6. 1982.

[5] BAUS R. BRULS A. Etude du comportement des ponts en acier sous l'action du trafic routier. Rapport CRIF. MT 145 - 1981.

[6] BRULS A. Mesures et interprétation des charges dynamiques dans les ponts - 2ème phase. Recherche CECA. Rapport EUR 8864 - 198.

[7] THONNARD, JANSS. Comportement à la fatigue des dalles orthotropes avec raidisseurs trapezoidaux. Rapport CRIF MT161-1985.

[8] BIGNONNET, JACOB, Mesures et interprétation des charges dynamiques dans les ponts. 3ème phase. Recherche CECA. 1989.

[9] BRULS, POLEUR, Traffic loads on road bridges. Equivalent loads effects - Eurocode on actions - Part 12 - Traffic loads on raod bridges - Subgroup fatigue - Appendix 2 - 1989.

[10] BRULS, Calibration of a load model for fatigue caculation. AIPC - Workshop. Remaining Fatigue Life of Steel Structures. Lausanne 1990.

Leere Seite
Blank page
Page vide

Fatigue Behaviour of Orthotropic Steel Bridge Decks

Comportement à la fatigue des dalles orthotropes de ponts en acier

Ermüdungsverhalten orthotroper Platten in Stahlbrücken

Stefano CARAMELLI
Prof. of Struct. Eng.
University of Pisa
Pisa, Italy

Maurizio FROLI
Researcher of Struct. Eng.
University of Pisa
Pisa, Italy

Pietro CROCE
Dr. Eng.
University of Pisa
Pisa, Italy

Luca SANPAOLESI
Prof. of Struct. Eng.
University of Pisa
Pisa, Italy

SUMMARY
Recently, some orthotropic steel bridge decks have suffered fatigue cracks. For a better knowledge of this problem, the European Community promoted and financed collective research work in which seven laboratories in six European countries participated. The Italian contribution to this research, deals with the experimental determination, on full scale specimens, of the fatigue behaviour of two types of welded connections of longitudinal stiffeners.

RÉSUMÉ
Récemment, quelques dalles orthotropes de ponts en acier ont montré des fissures de fatigue. Afin d'améliorer la connaissance de ce problème, la Communauté Européenne a encouragé et financé un programme de recherche auquel ont participé sept laboratoires de six pays européens. La contribution italienne, avait pour but de déterminer, de façon expérimentale et sur des éprouvettes en vraie grandeur, la résistance à la fatigue de deux types d'assemblages soudés de raidisseurs longitudinaux.

ZUSAMMENFASSUNG
In letzter Zeit wurden in den orthotropen Platten einzelner Stahlbrücken Rissbildungen infolge Ermüdung beobachtet. Um die Ursachen dieses Problems zu ergründen, wurde unter dem Patronat der Europäischen Gemeinschaft ein Forschungsprogramm zusammengestellt, an dem sieben Laboratorien aus sechs verschiedenen europäischen Ländern beteiligt waren. Der italienische Beitrag behandelt die an Bauteilen durchgeführte experimentelle Bestimmung des Ermüdungsverhaltens zweier verschiedener Schweissverbindungen von Längsrippen.

1. INTRODUCTION

The fatigue cracks appeared on some orthotropic decks of steel bridges after nearly twenty years of service life [1] showed that steel orthotropic decks are sensitive to fatigue problems and that their fatigue strength may not be directly estimated by means of the S-N curves proposed by the European codes which concern simple details used in steel constructions instead of the complex shaped connections of the orthotropic decks.

Beside that, the codified S-N curves are based on experimental results of little size specimens generally free from residual stresses patterns due to the welding procedures and probably less affected than the real scale complex shaped connections by local in the welds. But, as noticed by FISHER [2] and confirmated recently by YAMADA, KENDO, AOKI and KIKUCHI [3], CUNNINGHAME [4], AGERSKOV, BJØRNABAK-HANSEN [5] and others, lack of penetration, residual stresses and dimensions of the connected pieces are the factors that mostly influence the fatigue resistance of the joints.

In order to aquire a deeper knowledge on the static and fatigue behaviour of steel orthotropic decks, the ECSC promoted and financed the collective research programme: "Fatigue strength of orthotropic decks of steel bridges", third phase of the general programme: "Measures and interpretations of dynamical loads on bridges".

The research programme, concluded in 1989, was carried out by seven laboratories of six European countries among those, for Italy, the Istituto di Scienza delle Costruzioni of the University of Pisa.

The Italian programme foresaw the theoretical and experimental determination of the nominal stresses in those points of a real scale orthotropic deck more sensitive to a fatigue cracking risk and the execution of constant amplitude fatigue tests of stiffener to stiffener connections performed both on real scale ribs samples (type B specimens) and on the orthotropic deck panel previously used for the static test (type A specimen) [6].

This paper illustrates that part of the research dealing with the fatigue experiences.

2. FATIGUE TESTS ON TYPE B SPECIMENS

2.1 Description of the specimens and test modalities

The Fe 510C steel specimens, 200 mm long, consist of triangular cross section ribs built by welding a cold formed 6 mm thick steel plate to a top plate 600 mm wide and 12 mm thick. At middle span of each specimen, a type I or type II joint was shop executed reproducing the same working modalities provided for field execution. In figure 1 both type I joint and type II joint are illustrated, while in figure 2 the welding geometries S1÷S4 are shown.

In type I joints, the ribs are interrupted at a distance of about 200 mm astride the connection. The two limbs of the top plate - one of which has the backing strip welded to it (S1 welding) - are placed in such a way to get a root gap of about 6 mm, and thus automatically welded. The missing rib element is then inserted and manually welded in overhead position (backing strip weld S3 (fig. 3)).

In type II joints, the top plate is interrupted for about 200 mm. The stiffener webs are butt welded, with complete penetration, using S4 welding (fig. 4) which is manually executed with coated electrodes. First, the internal part of the ribs is welded in ascending vertical position, then one proceeds to the grooving of the external part and to the restarting of the weld in overhead position. The joining is completed with the insertion of the missing top plate portion, the execution of the S1 flat position welding and the manual overhead remaining wel-

ding S2 between the top plate and the ribs.

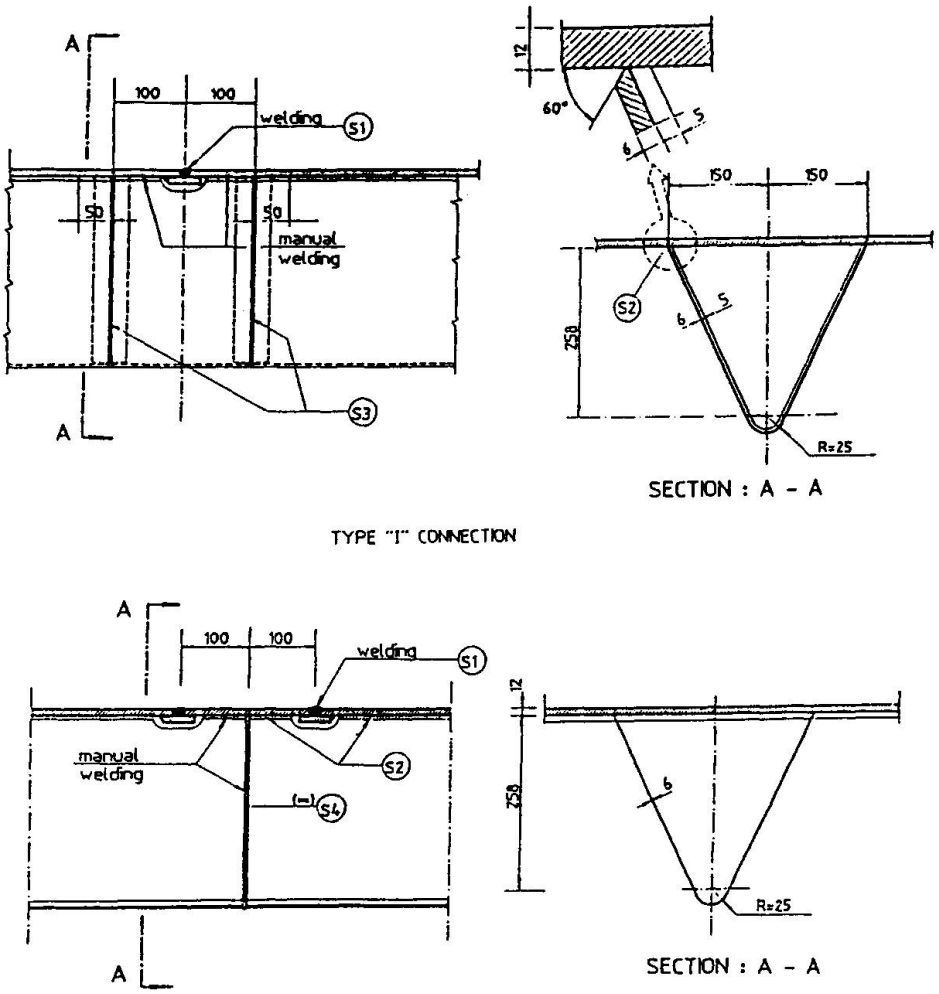

Fig. 1 Type I and type II stiffener to stiffener connections

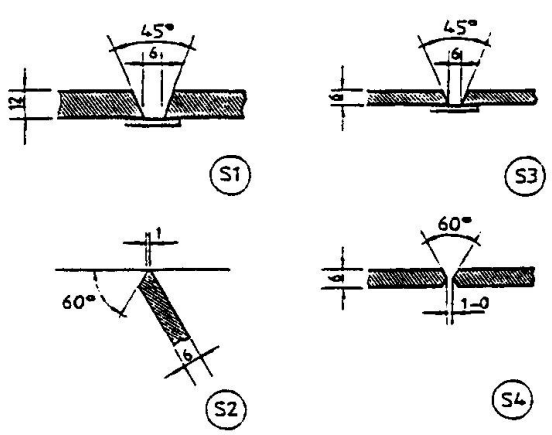

Fig. 2 Edge preparation

All the weldings have been checked by means of visual and magnetic controls. The butt weldings, moreover, have been 100 % X-raied and repaired where found (only one time) not acceptable according to the UNI 7278 Italian Standard.

The fatigue tests at constant stress amplitude, were carried out on nine type I joint specimens and on eight type II joint specimens.

The static test scheme is that of a simply supported beam, 2400 mm spanned, with the fatigue load applied at middle span by a pulsating hydraulic

jack acting with a frequency of 4 Hz.

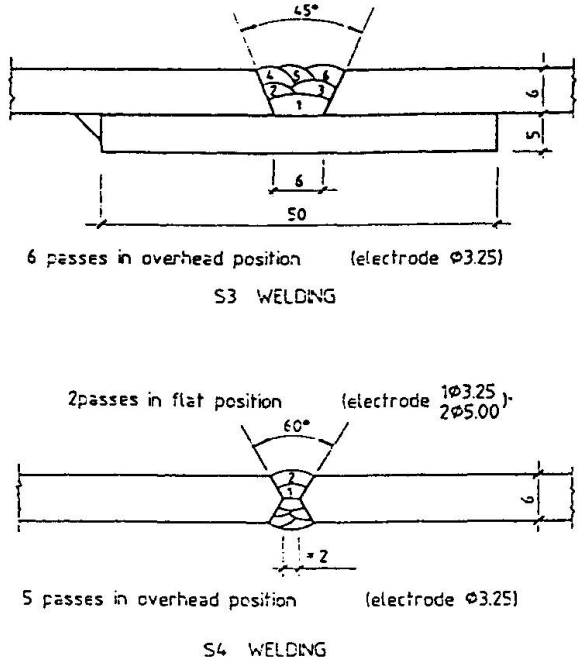

Fig. 3 S3 and S4 weldings

The load was applied on a rectangular neoprene strip 50 mm wide, 600 mm long and 10 mm thick, put between the moving jack and the top plate.

The stresses at the apex of the ribs were measured using electrical strain gauges, placed in a way that allowed the determination of the nominal stress amplitude excluding local peaks.

During the tests, the minimum nominal stress has been kept constantly at 1.5 KN/cm² for all the specimens.

Each test was interrupted at failure, recognized by the specimen's loss of stiffness (an increase of one centimeter of the maximum deflection under load), or when 8,000,000 cycles had been performed without any breaking.

2.2 Experimental results

The experimental results obtained on B specimens with type I joints and type II joints are respectively reported on the bilogarithmic S-N diagrams of figure 4 and 5 together with their mean life curves.

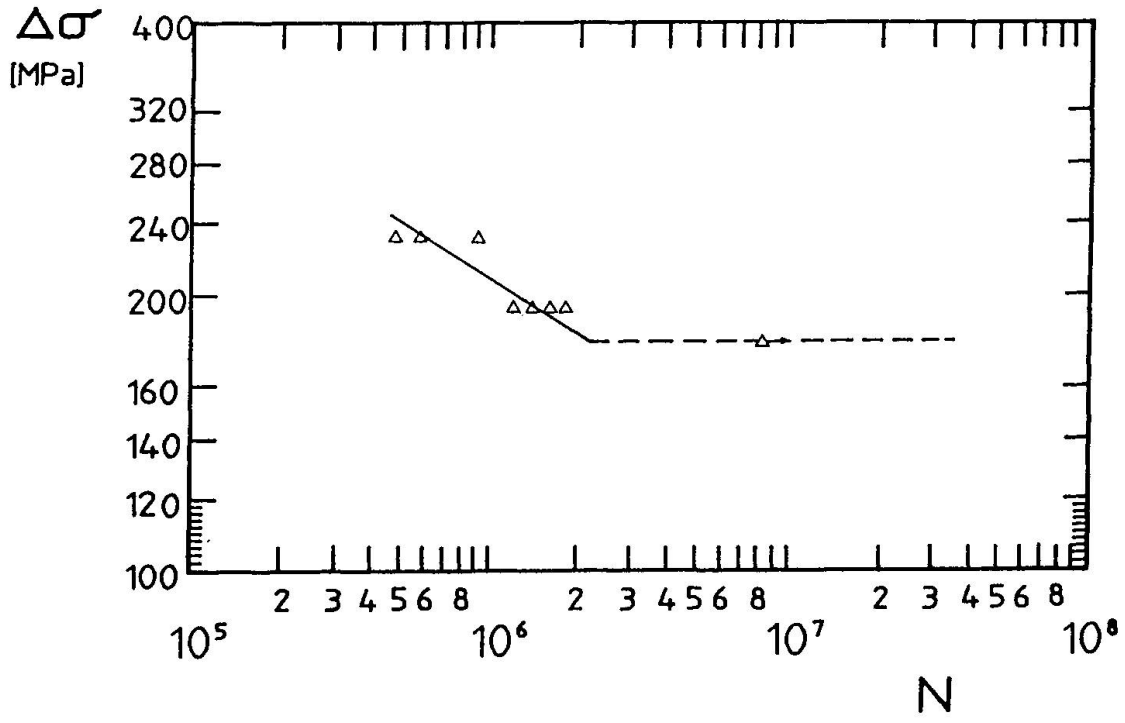

Fig. 4 Fatigue test results of type B specimens with type I joints

The two groups of results are then compared in the diagram of figure 6 from which the fatigue behaviour of type I joints appears to be better than that of

type II joints.

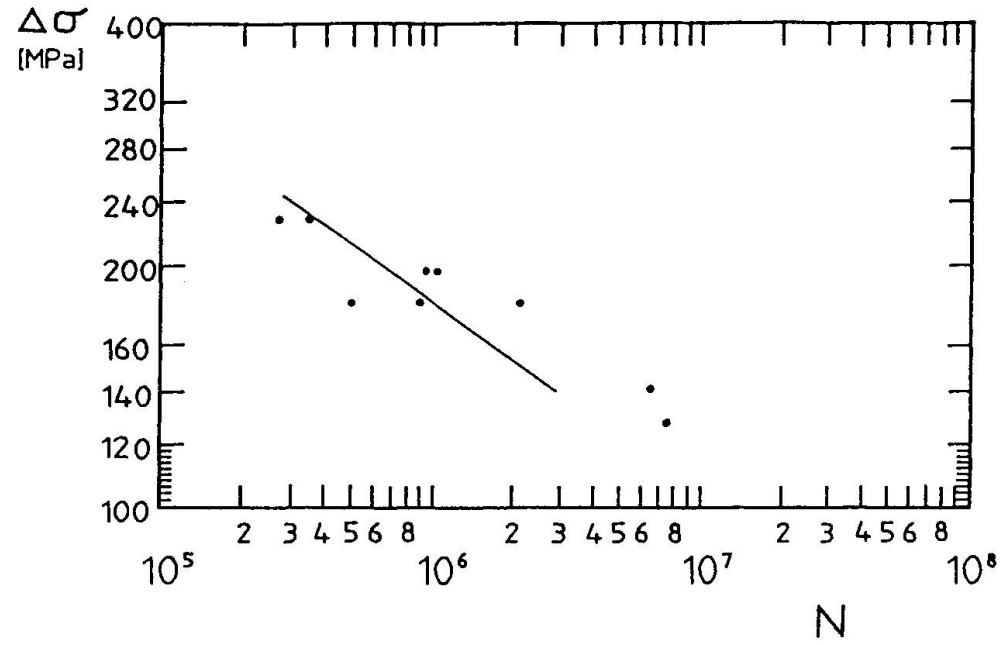

Fig. 5 Fatigue test results of type B specimens with type II joints

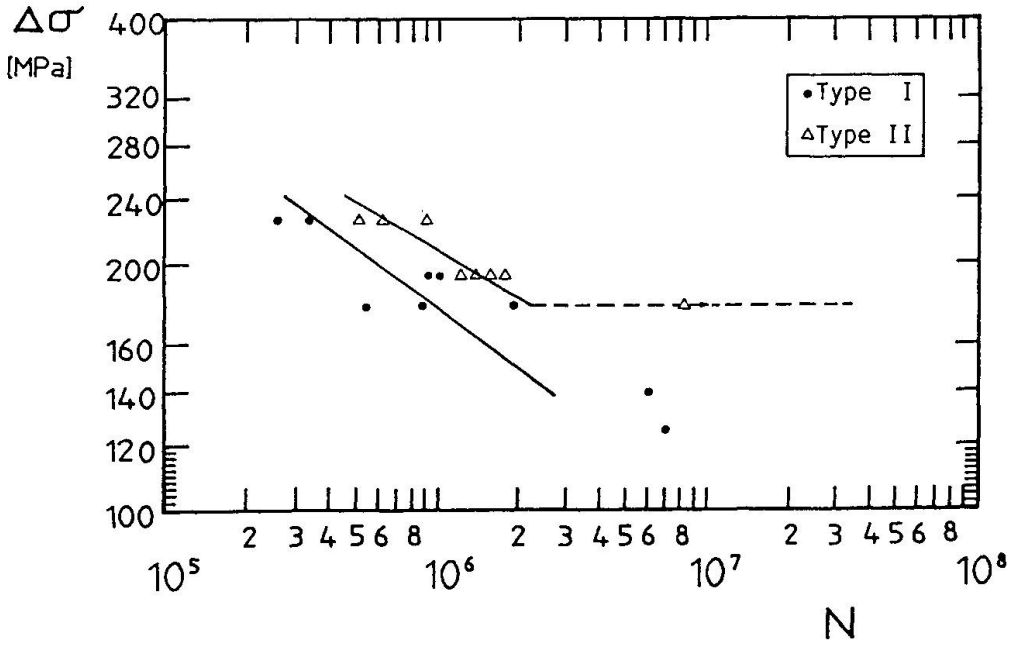

Fig. 6 Comparison between fatigue test results of type B specimens

3. COMPLEMENTARY TESTS

The previous result was rather unexpected because all the existing codes for fatigue design of steel structures classify backing strip welds in a lower position than complete penetration butt weldings (see for example [7]) and it is has also important consequences in the design practice because stiffener to stiffener connections with backing strip welds are more economic than the other welded connections.

In order to get a better understanding on the causes of the different behaviour of the two kinds of joints, it was decided to execute relaxation tests on type B specimens to control the residual stress levels and in the same time to perform a great number of fatigue tests on little size specimens provided with S3 and S4 weldings, for which residual stresses are negligible, to verify wether the different behaviour of the joints was to be attributed to the different types of weldings.

3.1 Residual stresses measurement in type B specimens

Residual stresses have been indirectly measured by means of mechanical relaxation tests executed on some type B specimens provided with type I and type II joints.

The test scheme is the same adopted for fatigue tests. During the test, some loading and unloading cycles have been performed until the steady cycle was reached. At each loading step the longitudinal strains at the lower apex of the stiffeners, close to the weld foot, have been measured.

Two typical load-strain curves related to type I joint and type II joint are reproduced in figure 7: it can be immediately noticed that residual stresses are almost absent in type I joints while one finds that they reach nearly 20 KN/cm² in type II joints.

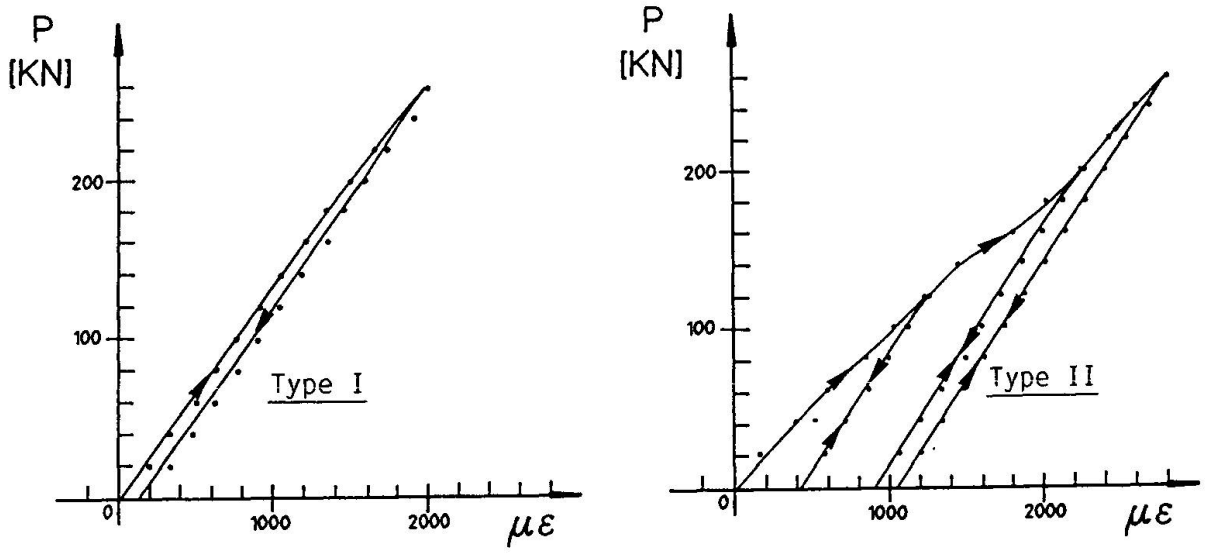

Fig. 7 Load-strain diagrams of the relaxation tests on type B specimens

3.2 Fatigue tests on welding specimens

The samples, 600 mm long, 35 mm wide and 6 mm thick, (figure 8) have been obtained by saw cutting two sheets 2000 X 300 X 6 mm of the same steel used for the stiffeners and welded together with the same modalities (operator position, number and sequence of passes, type of electrode) adopted for the S3 and S4 weldings used in type B specimens. Before cutting, the weldings have been submitted to the same checks executed for type B specimens without finding any defects.

In each specimen the surfaces of the cut have been ground to eliminate every stress concentration due to roughness and than fatigue tested under a tensile load pulsating sinusoidal with a frequency of 12 Hz, by means of a universal test machine Losenhausen UHP10. During the experience, the lowest tensile stress, kept constant for each specimen and equal to that of the type B speci-

mens, was 1.5 KN/cm².

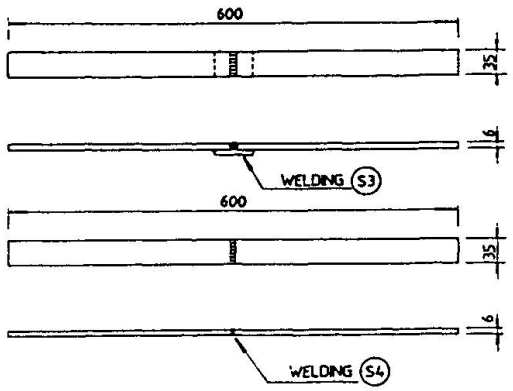

A number of 62 specimens have been tested: 31 with S3 weldings and 31 with S4 weldings.

The results are plotted on diagrams of figures 9 and 10, in which the mean S-N curves and the confidence band related with each group of results (fractile of 5% and of 95%), obtained following the ASTM E739-80, are reported too. It can be noticed that the two mean curves are practically coincident.

Fig. 8 Welding specimens

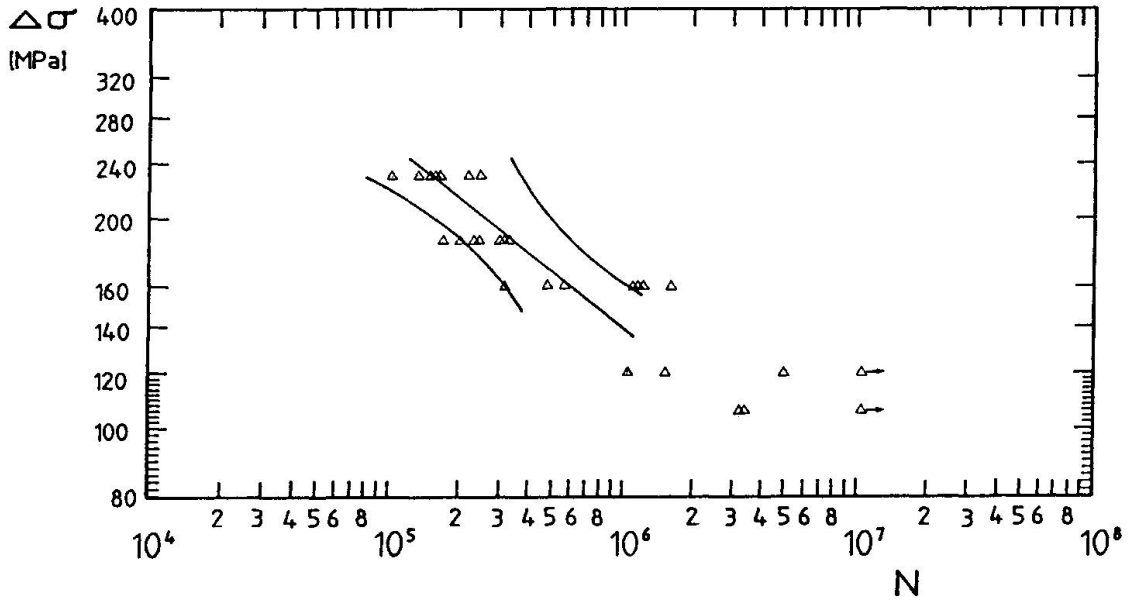

Fig. 9 Fatigue results on S3 welding specimens

4. FATIGUE TESTS ON TYPE A SPECIMENS

4.1 Description of the tests and test modalities.

In order to check the applicability of the fatigue results obtained on type B specimens to real deck joints, fatigue tests were carried out on two full scale orthotropic deck specimens provided with stiffener to stiffener type I joints which have been obtained by cutting crosswise along the central line the specimen used in the static test (type A specimen: see figure 11).

The test scheme is that of a plate with cantilever resting on two cross beams. The cantilever have been ballasted using two concrete blocks weighting totally 54 KN. The pulsating fatigue load, applied onto a 200X300 mm rectangular neoprene plate placed at middle span, induced a nominal stress delta at the lower apex of the central rib, close to the weld foot, equal to 22.5 KN/cm2 and a minimum stress of 1.5 KN/cm2, reference being the stress induced by the ballast and the self weight of the deck.

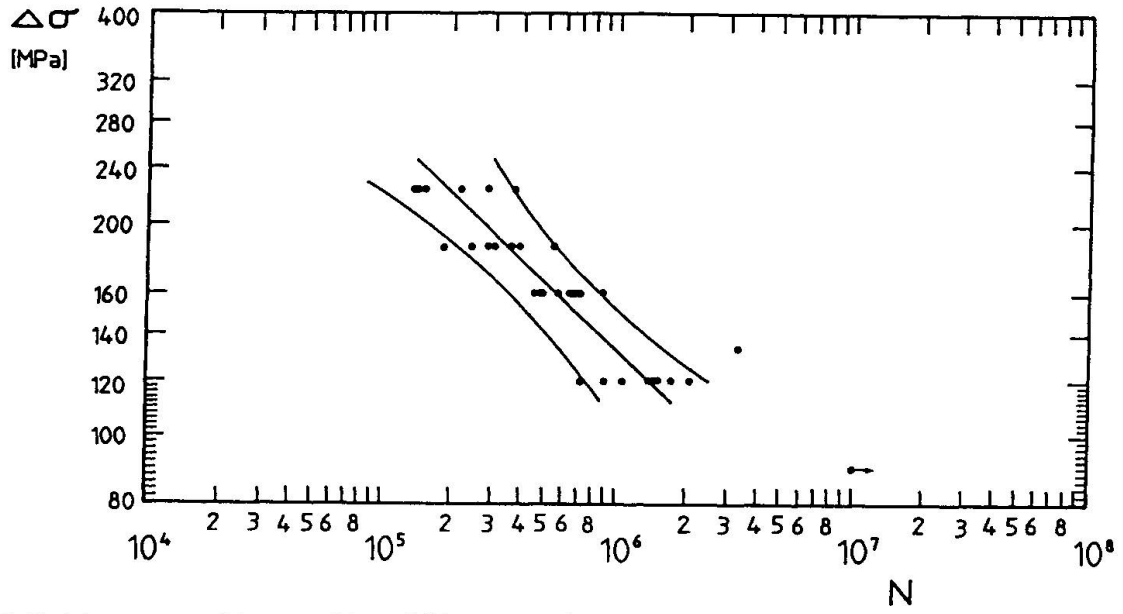

Fig. 10 Fatigue results on S4 welding specimens

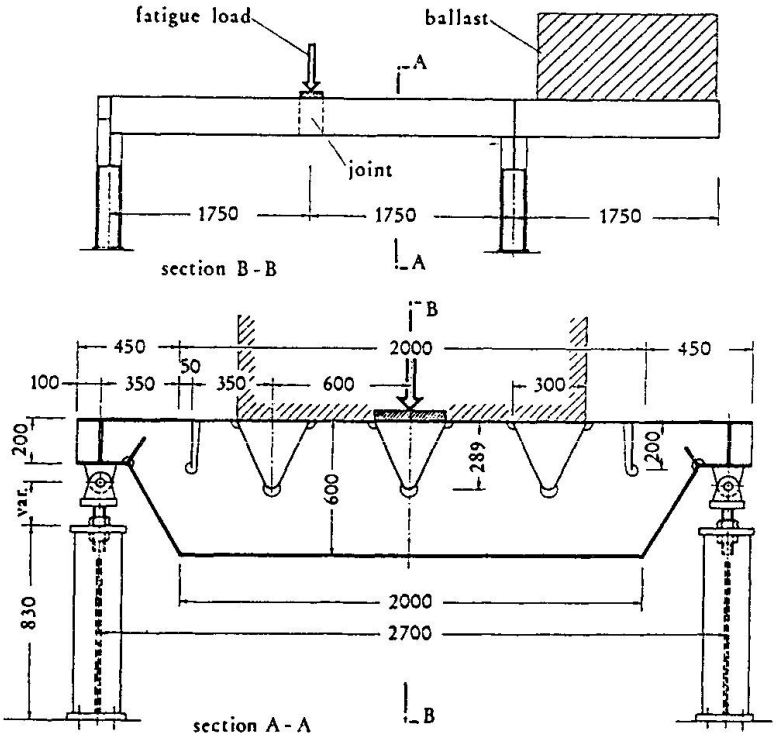

Fig. 11 Type A specimen

4.2 Experimental results

The first specimen failed after 240,000 cycles, the second one after 260,000 cycles. In both cases crack initiated in the weld at the apex of the rib and propagated in the weld too.

The comparison between the results obtained on the two types (A and B) of specimens reveals good accordance, within the normal dispersion limits. The lower fatigue strength revealed by type A specimens may be due to the residual stresses which in full scale orthotropic deck panels are to be expected higher than on simple ribs because of the greater stiffness of the deck.

5. CONCLUSIONS

The mean S-N curves of type B specimens and those regarding the welding specimens are compared in figure 12 where also the ECCS curves for backing strip weldings (class 71) and for full penetration weldings (class 80) are reported.

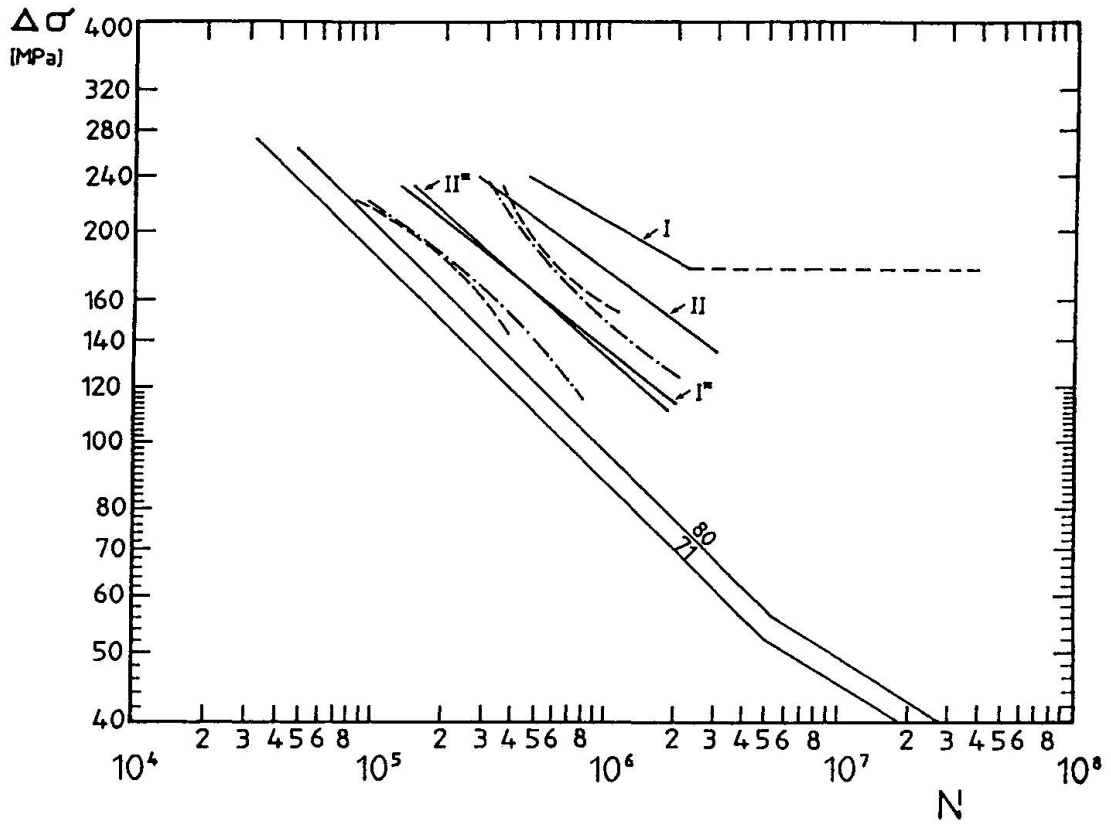

Fig. 12 Comparison between experimental results and ECCS curves

The S3 and S4 welding specimens have practically coincident fatigue strength and the 5% fractile curves of the two groups are situated both above ECCS curve 80. It can thus be concluded that the penalization of correctly designed and executed backing strip weldings, with respect to full penetration weldings, appears unjustified. On the contrary, type B specimens with type I joints have a higher fatigue life than that exhibited by type B specimens with type II joints (higher in both cases than that of the welding specimens because of the longer crack propagation life).

It follows then also that the fatigue life of the two types of joints does not dependent from the type of weldings (S3 or S4), if correctly executed and without defects, but depends from residual stresses.

Concluding, a distinction between joints, provided with backing strip weldings or full penetration weldings, based exclusively on the typology of the weldings and not taking into account the geometric features of the weldings themselves and the execution modalities of the connections is not justified. It is moreover not possible to assert "a priori" if it is safer or not to apply the present codified curves to complex details for which, at least for those most commonly used, it would be opportune to define specific S-N curves.

In our case, the authors mean that also backing strip weldings if correctly designed and executed, could be inserted in ECCS class 80.

Some aspects of the problem, such as more precise evaluation of residual stres-

ses, remain still not completely clarified and the authors intend to dedicate on them their future research work.

REFERENCES

1. WOLCHUK R., Lessons from weld cracks in orthotropic decks on three european bridges. ASCE Journ. Struct. Eng., 1990.

2. FISHER J.W., Fatigue and fracture in steel bridges. Wiley & Sons, New York, 1984.

3. YAMADA K., KONDO A., AOKI H., KIKUCHI Y., Fatigue strenght of field-welded rib joints of orthotropic steel decks. IIW Doc. XIII-1282-88, Department of Civil Engineering, Nagoya, 1988.

4. CUNNINGHAME J.R., Steel bridge decks: fatigue performance of joints between longitudinal stiffeners. TRRL Laboratory Report 1066, Crowthorne, 1982.

5. AGERSKOV H., BJØRNBACK-HANSEN J., Fatigue investigation on orthotropic steel bridge deck. IIW Doc. XIII-1195-86, Department of Structural Engineering, Lyngby, 1986.

6. CARAMELLI S., CROCE P., FROLI M., SANPAOLESI L., Misure ed interpretazioni dei carichi dinamici sui ponti. III fase. Resistenza a fatica delle piastre ortotrope da ponte in acciaio. Relazione tecnica finale della Ricerca CECA N.7210-KD/411, Istituto di Scienza delle Costruzioni, Pisa, 1989.

7. CECM Recommandations pour la vérification à la fatigue des structures en acier. Construction Métallique, 1987.

Fatigue Assessment of Orthotropic Steel Decks of Box Girder Bridges

Comportement à la fatigue des dalles orthotropes en acier de ponts en caisson

Einschätzung des Ermüdungsverhaltens orthotroper Stahlfahrbahnplatten von Hohlkasten-Brücken

Kentaro YAMADA
Professor
Nagoya University
Nagoya, Japan

Kentaro Yamada, born 1946, received his civil engineering degree at Nagoya University, and PhD at University of Maryland, MD, USA. Since then, he has been involved in fatigue tests of welded structures, application of fracture mechanics, and field measurement of service stresses of highway bridges.

SUMMARY

This report shows a case study on fatigue assessment of orthotropic steel decks of box girder bridges typically used for urban elevated highway systems in Japan. Cumulative fatigue damage for several welded joints on the bridge are computed using design wheel loads and truck models that represent service truck traffic.

RÉSUMÉ

Cet exposé présente une étude de cas sur le comportement à la fatigue des dalles orthotropes en acier de ponts en caisson typiques des autoroutes urbaines surélevées au Japon. Le cumul du dommage en fatigue pour plusieurs joints soudés du pont a été estimé à l'aide des charges de roue normalisées et des modèles de camion représentant le trafic usuel de poids lourds.

ZUSAMMENFASSUNG

Der vorliegende Bericht behandelt eine Fallstudie zur Einschätzung des Ermüdungsverhaltens orthotroper Stahlfahrbahnplatten von Hohlkasten-Brücken, wie sie in Japan für städtische Hochstrassen verwendet werden. Für Norm-Radlasten und Lastmodelle, die den Schwerverkehr darstellen, wird die Schadensakkumulation an verschiedenen geschweissten Verbindungen der Brücke berechnet.

1. INTRODUCTION

The orthotropic steel decks are susceptible to fatigue cracking when they are subjected to extremely heavy truck traffics [1, 2]. Actually, a few fatigue cracks have been observed in orthotropic steel decks, some of which are shown in Fig.1. It is due to the fact that the decks support directly the wheel loads that sometimes exceed the design ones. A load survey in Japan showed that there were trucks of about 378 kN (38 tons) and trailer trucks of about 666 kN (68 tons) [4], while the the design truck loads are based on 196 kN (20 tons, T-20 truck) and 421 kN (43 tons, TT-43 truck), respectively[5].

This report shows a case study on fatigue assessment of orthotropic steel decks of box girder bridges typically used for urban highway systems. Cumulative fatigue damages for several welded joints are computed for the design wheel loads and for a series of model trucks representing actual truck traffic observed in the Hanshin Expressway [4], one of the major elevated urban highway systems in Japan.

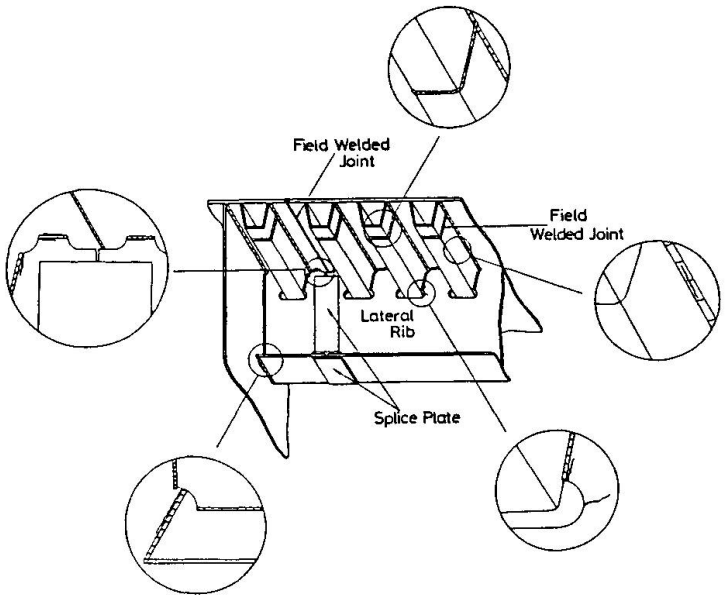

Fig.1 Example of fatigue cracks in orthotropic steel deck

2. FATIGUE ASSESSMENT OF ORTHOTROPIC STEEL DECKS

Fatigue assessment of orthotropic steel decks may be carried out by one of the following procedures.

(1) Assessment according to the design specifications

The current design specifications for the highway bridges [5] require fatigue assessment only for the orthotropic steel decks. The specifications give a few structural details and their fatigue allowable stress ranges corresponding to two million cycles. The stress ranges due to wheel loads should be less than these values [9]. The procedure is simple and feasible to most highway bridges. However, it seems insufficient when the decks are subjected to extremely heavy truck traffic with some overloadings.

(2) Assessment due to fatigue design load

An alternative way is to use an equivalent fatigue design loads, if any, which simulate the service loading condition. In order to compute the equivalent fatigue design loads, the weight and the frequency of the service loads are necessary. If the equivalent fatigue design loads are given as the fraction α of the static design loads, results for static design can be conveniently used for fatigue

assessment. The factor α is affected by the service load condition and the influence lines of the details of interest.

(3) Assessment using service loads

It seems more accurate when one can apply directly the service loads to the orthotropic steel decks and to count the resulted stress cycles. The stress cycles can be counted by the rainflow counting method and apply the Miner's cumulative damage rule. Because it needs accurate service loading prior to the computation and the computation is rather complex, it seems unrealistic to be used in design. However, the computed fatigue life seems reliable, when the reasonable S-N diagrams for the structural details are available.

(4) Assessment using measured service stresses

Recent development of so-called "Histogram Recorder" made it rather easy to measure service stresses in existing structures. Numerous measurements of service stresses in steel bridges were carried out throughout Japan [3]. The measured stress histograms can be used directly for fatigue assessment using the Miner's cumulative damage rule.

3. CASE STUDY ON FATIGUE ASSESSMENT OF ORTHOTROPIC STEEL DECKS

3.1 General Procedure

A part of a typical box girder bridge with orthotropic steel decks was selected and analyzed by grid theory. Design truck loads, T-20 and TT-43 trucks, and model truck loads that represent the service load condition are applied to the influence surfaces of the bending moments respectively to compute the resulting stress waves. The stress waves were then counted by the rainflow counting method and fatigue damages were computed by Miner's rule using appropriate design S-N curves.

3.2 Structural Analysis of Orthotropic Steel Decks

The model of the orthotropic steel decks was selected from "Typical Examples of Box Girder Bridge with Orthotropic Steel Decks," proposed by the Hanshin Expressway [6]. The bridge is consisted of two box girders of 72 m span carrying four-lane traffics, two lanes in each direction, as shown in Fig.2a. The grid analysis was carried out for a section of 12 m long with two cross beams and three lateral ribs of 3 m apart, as shown in Fig.2b. Influence surfaces were obtained for the structural details of interest.

The followings are the assumptions in the analysis.

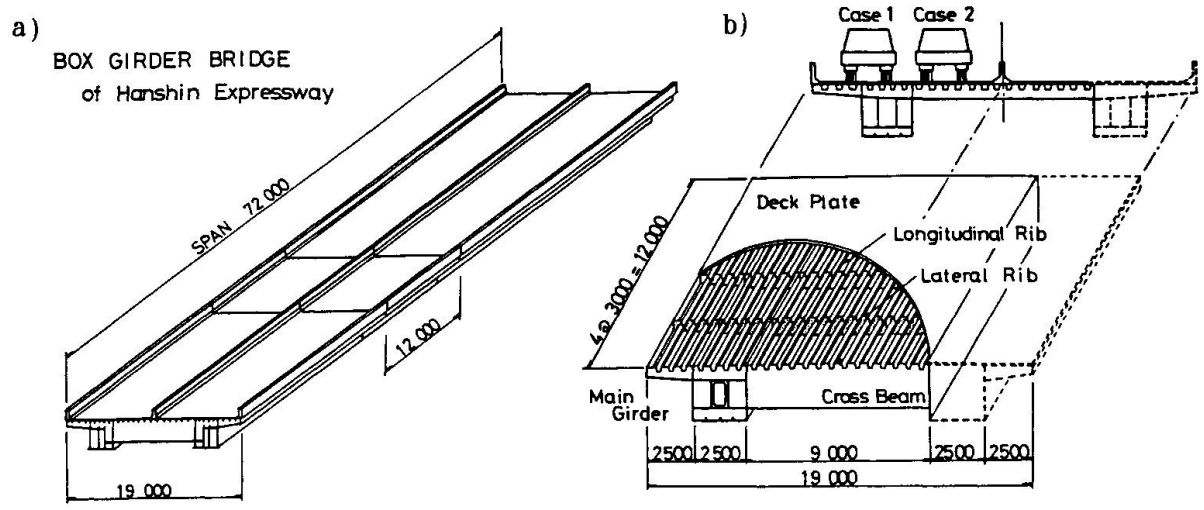

Fig.2 Analytical model of box girder bridge with orthotropic steel deck

(1) The orthotropic steel decks were assumed as a grid that consists of trapizoidal ribs, lateral ribs, cross beams and main girders.
(2) A box girder were divided into two I beams, each supporting the orthotropic steel decks at the upper end of the web.
(3) The effective widths of the decks were computed according to the Design Specification of the Highway Bridges [5].

3.3 Structural Details

Fatigue assessments were carried out for six welded joints, as shown in Fig.3. The arrows in Fig.3 indicate the stress direction. The design S-N curves were selected from the fatigue design recommendation for the welded structure proposed by the European Convention for the Constructional Steelwork (ECCS) [7]. The detail categories are numbered in the recommendation according to their fatigue strength at two million cycles. The structural details and their detail categories used in the computation were as follows.
(1) longitudinal fillet welds connecting trough ribs to deck; stress category 100.
(2) lower ends of fillet welds between trough ribs and web of the lateral rib subjected to stresses in the longitudinal direction; stress category 80.
(3) lower ends of fillet welds between trough ribs and lateral ribs with load carrying fillet welds; stress category 71 for toe crack and stress category 36 for root crack.
(4) upper end of the fillet welds between trough ribs and lateral ribs; stress categories 71 and 36.
(5) end of fillet welds between web of the lateral ribs and deck; stress category 71.
(6) full penetration groove welds between lateral ribs and web of main girder; stress category 71.

The fatigue assessments were carried out for the details in the structures that showed the maximum range of bending moment, when the design loads, T-20 and TT-43, moved on slow lane and passing lane. Stresses were computed by the beam theory.

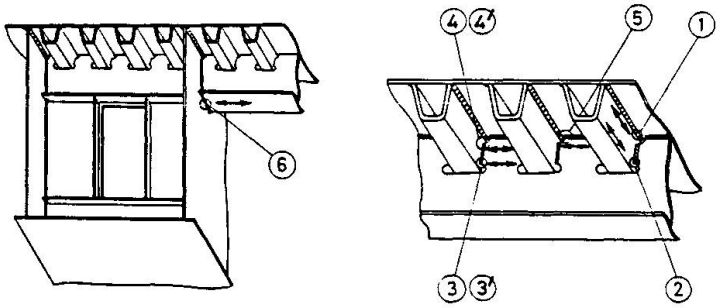

Fig.3 Welded joints for fatigue assessment

3.4 Computation of Stress Waves

The design truck loads and model truck loads were applied to the influence surfaces computed by the grid theory. The following assumptions were made in the analysis.
(1) The wheel loads were assumed as concentrated loads and the impact factor was not considered.
(2) The wheel loads passed on the same line, and the distribution in lateral direction was not considered.
(3) A single truck passes on the deck at a time.
(4) The truck passes either on the slow lane or the passing lane.
The stress ranges and the number of cycles were counted for those stress waves using rainflow counting method.

3.5 Design S-N Diagrams

The Miner's cumulative damage D can be expressed as follows:

$$D = \sum_{i=1}^{k} n_i/N_i \qquad (1)$$

where n_i is the number of cycles of stress ranges σ_{ri}, N_i is the design fatigue life of the detail at σ_{ri} obtained from design S-N diagram, and k is the number of stress ranges of variable amplitude.

The following three types of design S-N diagrams can be used, as shown in Fig.4 [7, 8].

I: A single S-N diagram of slope m = 3 is used. (Modified Miner's rule)
II: When stress ranges are below the constant amplitude fatigue limit of the detail at five million cycles, slopes of the S-N diagrams are changed into m = 5.
III: When stress ranges are below the cut-off limit at 100 million cycles, these stress ranges are neglected.

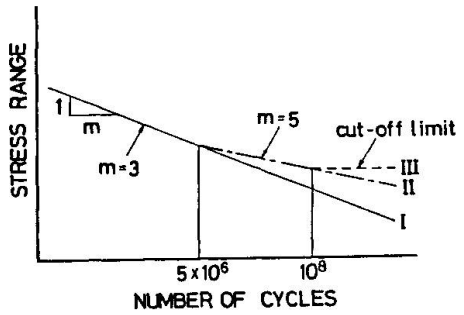

Fig.4 S-N diagram used for fatigue damage analysis

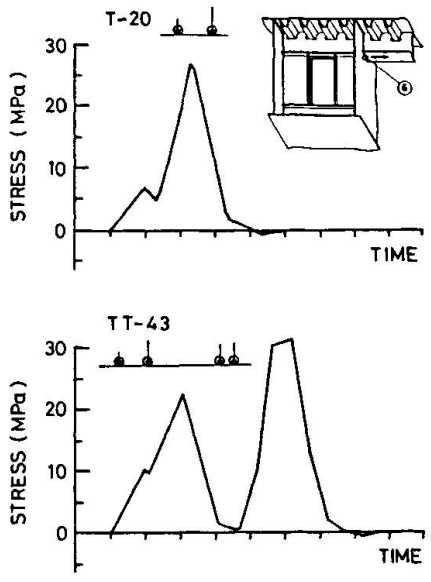

Fig.5 Stress wave due to model truck (lateral rib)

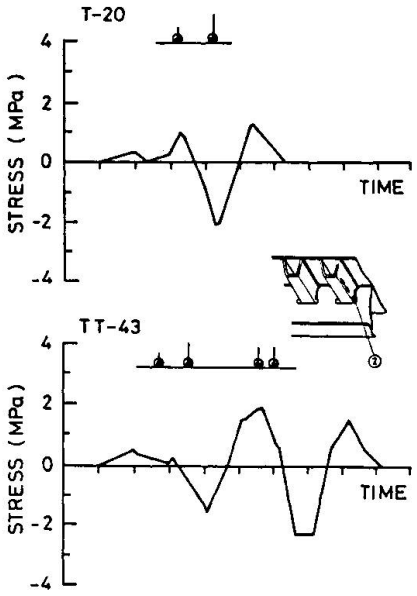

Fig.6 Stress wave due to model truck (longitudinal rib)

4. FATIGUE ASSESSMENTS FOR DESIGN TRUCKS

4.1 Stresses due to Design Truck, T-20 and TT-43

Computed stresses at the lateral ribs (detail No.6) due to T-20 and TT-43 trucks are shown in Fig.5. The T-20 truck has a wheel base of 4 m, which results in one large stress range per truck. On the contrary, the TT-43 truck gives two stress ranges per truck, because the distance between the front axle and the rear axle is about 7.8 m, and it is larger than the size of the influence surface of the details. The stresses at the longitudinal ribs (Detail No.2) are shown in Fig.6. The influence surface of this detail is small, and the fluctuating stresses appear for each passage of wheel.

4.2 Fatigue Damages

In order to compute fatigue damage due to the design trucks, design life and the number of design trucks passing on this bridge must be assumed. In this analysis

Table 1 Computed fatigue damage for design loads

Joint No.	Joint Classification (ECCS)	S-N Diagram	Fatigue Damage during 50 Years (4260/day/lane)		
			T-20		TT-43
			Case 1	Case 2	Case 2
①	100	I II III	no no 0.0	no no 0.0	no no 0.0
②	80	I II III	no no 0.0	3.0×10^{-3} no 0.0	6.6×10^{-3} no 0.0
③	71	I II III	no no 0.0	no no 0.0	no no 0.0
③'	36	I II III	no no 0.0	no no 0.0	1.2×10^{-3} no 0.0
④	71	I II III	no no 0.0	3.4×10^{-3} no 0.0	7.2×10^{-3} no 0.0
④'	36	I II III	no no 0.0	4.2×10^{-2} no 0.0	9.1×10^{-2} 2.1×10^{-3} 0.0
⑤	71	I II III	no no 0.0	6.0×10^{-3} no 0.0	1.3×10^{-2} no 0.0
⑥	71	I II III	no no 0.0	2.33 0.65 0.0	4.96 1.66 1.40

no : Fatigue Damage less than 10^{-3} is considered no Fatigue Cracking Condition.

it was assumed that the design life was 50 years and the number of daily design trucks was 4260. It corresponds to the trucks that constitute 14.2 percent of the 30,000 vehicles passing daily on one lane.

The computed fatigue damages in 50 years of life span for six structural details are summarized in Table 1. When the T-20 truck passes on the slow lane (case 1),

the computed fatigue damages are less than 0.001. Although various assumptions are made in the analysis, one can safely conclude that these details are not susceptible to fatigue, with the design trucks passing on the slow lane.

The following discussion forcus only on the case 2, where the design trucks pass on the passing lane. The computed fatigue damages due to the TT-43 truck are about 2 to 2.5 times that of the T-20 trucks. It is due to the fact that the computed stresses are about the same for both trucks, while the TT-43 truck gives the number of cycles about twice of that from T-20 truck.

The lateral ribs connected to the main girder webs showed rather large fatigue damage, especially when the modified Miner's rule (S-N diagram I) is used. This is maybe because a diaphragm is usually fabricated in the box girder, outside of which cross ribs are welded and thus provides a structural discontinuity point for the cross ribs.

5. FATIGUE ASSESSMENT FOR SERVICE LOADS

5.1 Model Trucks Simulating Service Loads

Weights of all passing vehicles were measured for 24 hours by the Hanshin Expressway Public Authority in 1982 [4]. As shown in Table 2, about 72,000 vehicles passed, and 14.2 percent of them were trucks. The maximum weight of the trucks were 236 kN (24.1 tons) for the trucks with two axles, 370 kN (37.8 tons) with three axles, and 670 kN (68.4 tons) for trailer trucks. About 38 percent of the two axle trucks and about 49 percent of the trailer trucks weighed more than the design T-20 truck (196 kN or 20 tons, two axles). About 5 percent of trailer trucks weight more than the design TT-43 truck (421 kN or 43 tons, four axles).

Table 2 Classification of vehicles passing on Hanshin Expressway

Traffic Classification			Daily Traffic	Percentage
Large Vehicle	2 axles		1,630	2.3 %
	Tandem axle	3 axles(1)	4,926	6.8 %
		3 axles(2)	2,019	2.8 %
		4 axles	152	0.2 %
	Trailer		1,565	2.2 %
	Total		10,292	14.2 %
Middle Vehicle			12,913	17.8 %
Car			49,189	67.9 %
Total			72,394	100.0 %

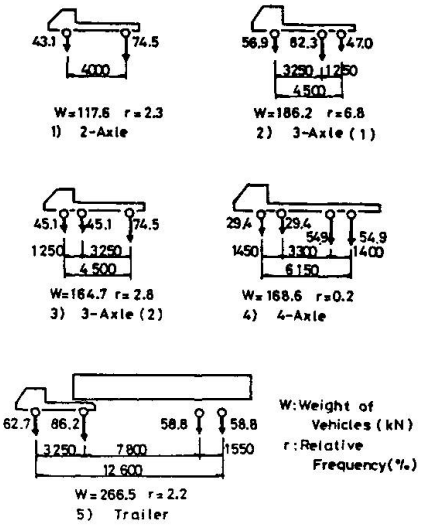

Fig.7 Model trucks representing service loading

The observed trucks were then re-grouped into five model trucks, as shown in Fig.7. They were; 1) two-axle truck; 2) three-axle truck with two rear axles; 3) three-axle truck with two front axles; 4) four-axle truck; and 5) trailer truck. The weights of the model trucks were computed using Eq.2.

$$W = \Sigma \ (f_i \ . \ W_1^m)^{1/m} \qquad (2)$$

where W_i is the measured truck weights and f_i is its relative frequencies. When m = 3 is used, W becomes so-called equivalent truck weights using modified Miner's rule. The wheel bases were also measured, and their mean values were computed, as shown in Fig.7. Each axle weight was also determined from the average axle weight ratio.

5.2 Computed Fatigue Damages and Equivalent Loads

The model trucks were applied to the passing lane, and fatigue damages for the six structural details were computed. It was assumed that the design life was 50 years and the average daily traffic was 30,000 vehicles in one lane. The results are summarized in Table 3. In general, for each structural detail, the three axle trucks with one front axle gives the most fatigue damages, owning to its relative frequency. The trailer trucks also gives large fatigue damages, because their weights are relatively large, and they usually gives more than two major stress ranges per truck.

Table 3 Computed fatigue damage due to model trucks measured by Hanshin Expressway Public Authority

Joint No.	S-N Diagram	Fatigue Damage during 50 years (30,000/day/lane)						Model Load (kN)
		2 axles (2.3%)	3 axles(1) (6.8%)	3 axles(2) (2.8%)	4 axles (0.2%)	Trailer (2.2%)	Total (14.2%)	
①	I	6.7×10^{-7}	4.3×10^{-6}	8.4×10^{-7}	2.2×10^{-7}	3.7×10^{-6}	9.7×10^{-6}	110
	II	2.2×10^{-11}	2.9×10^{-10}	2.5×10^{-11}	1.8×10^{-11}	3.2×10^{-10}	6.8×10^{-10}	
	III	0.0	0.0	0.0	0.0	0.0	0.0	
②	I	3.5×10^{-5}	2.3×10^{-4}	4.5×10^{-5}	1.2×10^{-5}	2.0×10^{-4}	5.2×10^{-4}	110
	II	1.7×10^{-8}	2.2×10^{-7}	1.9×10^{-8}	1.4×10^{-8}	2.5×10^{-7}	5.2×10^{-7}	
	III	0.0	0.0	0.0	0.0	0.0	0.0	
③	I	9.6×10^{-7}	1.1×10^{-5}	1.5×10^{-6}	2.1×10^{-7}	3.6×10^{-6}	1.7×10^{-5}	144
	II	5.0×10^{-11}	1.3×10^{-9}	9.8×10^{-11}	2.1×10^{-11}	3.0×10^{-10}	1.8×10^{-9}	
	III	0.0	0.0	0.0	0.0	0.0	0.0	
③'	I	1.2×10^{-5}	1.3×10^{-4}	1.9×10^{-5}	2.7×10^{-6}	4.5×10^{-5}	2.1×10^{-4}	143
	II	3.4×10^{-9}	9.0×10^{-8}	6.6×10^{-9}	1.4×10^{-9}	2.0×10^{-8}	1.2×10^{-7}	
	III	0.0	0.0	0.0	0.0	0.0	0.0	
④	I	7.6×10^{-5}	8.3×10^{-4}	1.2×10^{-4}	1.7×10^{-5}	2.9×10^{-4}	1.3×10^{-3}	142
	II	7.3×10^{-9}	1.9×10^{-6}	1.4×10^{-7}	3.0×10^{-8}	4.3×10^{-7}	2.6×10^{-6}	
	III	0.0	0.0	0.0	0.0	0.0	0.0	
④'	I	9.5×10^{-4}	1.0×10^{-2}	1.5×10^{-3}	2.1×10^{-4}	3.6×10^{-3}	1.6×10^{-2}	142
	II	4.9×10^{-6}	1.3×10^{-4}	9.6×10^{-6}	2.0×10^{-6}	2.9×10^{-5}	1.8×10^{-4}	
	III	0.0	0.0	0.0	0.0	0.0	0.0	
⑤	I	1.3×10^{-4}	1.5×10^{-3}	2.2×10^{-4}	2.2×10^{-7}	5.1×10^{-4}	2.4×10^{-3}	144
	II	1.9×10^{-7}	5.0×10^{-6}	3.7×10^{-7}	1.8×10^{-11}	1.1×10^{-6}	6.7×10^{-6}	
	III	0.0	0.0	0.0	0.0	0.0	0.0	
⑥	I	0.04	0.43	0.06	7.2×10^{-3}	0.14	0.64	127
	II	2.6×10^{-3}	0.06	4.5×10^{-3}	7.3×10^{-4}	0.01	0.08	
	III	0.0	0.0	0.0	0.0	0.0	0.0	

( ) : Relative Frequency

The structural detail No.6, which is the lateral ribs welded to the main girders, showed the largest fatigue damage. This was the same trend as in the case of design truck loads. However, the fatigue damage was 0.64 in 50 years, even when the modified Miner's rule is used. It implies that the detail is not susceptible

to fatigue crackings, when the loading pattern and the number of vehicles remain the same over the assumed design life of 50 years.

The model truck loads give smaller fatigue damages than the design T-20 or TT-43 truck loads. It implies that the weight of the design truck can be reduced by the factor α, when one wants to obtain the same fatigue damages as the model loads. The reduced design truck loads are computed and summarized as equivalent loads in Table 3. It is concluded that the equivalent loads are between 54 and 75 percent of the weight of the T-20 trucks.

5.3 Fatigue Damage due to Different Daily Trucks and Truck Ratio

Fatigue damages were also computed for different daily traffic and different truck ratio. The weights and the wheel bases as well as the relative frequencies of the model trucks were assumed unchanged during the design life of 50 years. The fatigue damages were computed for the structural detail No.6, and plotted in Fig.8. The fatigue damages were mainly caused by the large vehicles, and the damage does not exceed unity when the total vehicles are 10,000 and the trucks are 40 percent of them (i.e. 4,000 trucks per day). On the contrary, when the total

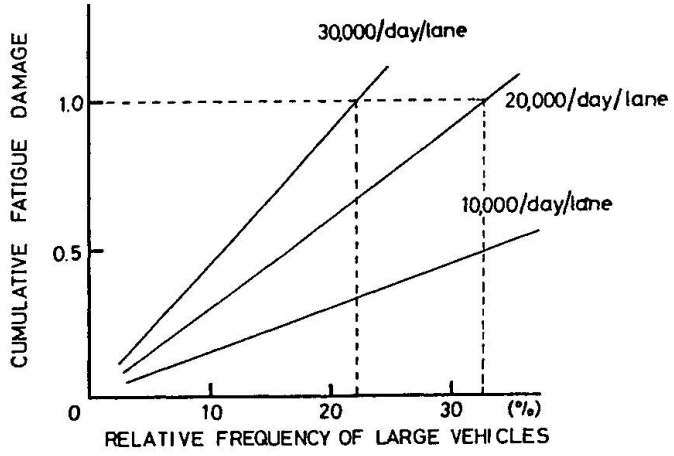

Fig.8 Effect of relative frequency of trucks on fatigue damage

vehicles is about 30,000, and the trucks are over 22 percent (i.e. 6,600 trucks per day), the damage exceeds unity. If the bridge carries 30,000 vehicles per day per lane and 44 percent of them are trucks, fatigue damage might exceed unity within 25 years at this detail.

6. SUMMARY OF FINDINGS

Fatigue damages were computed for the typical box girder bridge with the orthotropic steel decks using the design T-20 and TT-43 truck loads and the model truck loads. A part of the decks was analyzed and the stress waves were obtained by using grid thoery. The fatigue damages were computed for six welded details in the structure using the Miner's cumulative damage rule. The followings summarize the findings.

(1) The computed fatigue damages are normally larger when the trucks pass on the passing lane than on the slow lane.

(2) The lateral ribs welded to the webs of the main box girders showed the largest fatigue damage when the design trucks were applied.

(3) The model trucks, computed from the measured weights and the wheel bases by the Hanshin Expressway Public Authority, showed less fatigue damages than that due

to the design trucks. The fatigue damages were less than unity for all structural details with the current traffic condition, such as 30,00 vehicles per lane and 14.2 percent truck ratio.
(4) However, when the daily vehicles increase or when the number of trucks increase over the present condition, the computed fatigue damage may exceed the unity.
(5) The TT-43 truck gives about 2 to 2.5 times more fatigue damage than the T-20 truck, because the former gives two major stress ranges per truck for structural details of the orthotropic steel decks.
(6) When compared with the T-20 design trucks, the model trucks that represent the service condition of the Hanshin Expressway give fatigue damages between 0.16 and 0.40 depending on the structural details and the truck types. Therefore, the weight of the equivalent model trucks are about 54 to 75 percent that of the design T-20 truck.

ACKNOWLEDGEMENT

The author express his sincere appreciation to Dr. A. Kondo of Meijo University, Dr. H. Terada of the Yokogawa Bridges works, Mr. K. Hasegawa of Mitsubishi Heavy Industries, Mr. Ma Zhiliang of Nagoya University and Mr. H. Ishizaki of Hanshin Expressway Public Authority for their valuable discussion and suggestion throughout the study. A majority of this report was already published in Ref. 11 in Japanese and in Ref. 12 in English. The research was carried out under the Grant -in Aids for scientific research of Ministry of Education, Science and Culture.

REFERENCES

1. CUNINGHAM, J.K.: Strengthening fatigue prone details in a steel bridge deck, International Conference on Fatigue of Welded Constructions, Brighton, April 1987.
2. Subcommittee on Fatigue of Steel Orthotropic Deck; Fatigue of orthotropic steel bridge deck, Proc. of JSCE, No.410/I-12, 1989.10.
3. YAMADA, K. and MIKI, C.; Recent research on fatigue of bridge structure in Japan, Journal of Constructional Steel Research, Vol.13, 1989.
4. Hanshin Expressway Public Authority; Survey on service loads on the Hanshin Expressway, 1984.
5. Japan Road Association; Design specifications for highway bridges, 1980.
6. Hanshin Expressway Public Authority; Typical examples of box girder bridges with orthotropic steel decks, 1988.3.
7. European Convention for Constructional Steelwork; ECCS recommendations for fatigue design of Steel Structures, 1985.
8. British Standard Institution; Steel, concrete and composite bridges, Part 10, Code of Practice for Fatigue, 1980.
9. KUNIHIRO, T. and FUJIWARA, M.; Conventional design calculation of orthotropic steel decks using the orthotropic plate theory, Report of PWRI, No.137, 1969.
10. FUJIWARA, M. et al.; Survey on connection between lateral ribs and longitudinal ribs of orthotropic steel decks, Annual Convention of JSCE, No.43, 1988.
11. HASEGAWA, K. et al.; Fatigue assessment of orthotropic steel deck of box girder bridge, Journal of Structural Eng., JSCE, Vol.34A, 1989.3.
12. YAMADA, K. et al.; Fatigue assessment of orthotropic steel decks of box girder bridge, Pacific Structural Steel Conference, STEEL 2001, Gold Coast, 1989.